LOGISTIC CELLULAR AUTOMATA

A THESIS SUBMITTED TO
THE GRADUATE SCHOOL OF ENGINEERING AND SCIENCE
OF BILKENT UNIVERSITY
IN PARTIAL FULFILLMENT OF THE REQUIREMENTS FOR
THE DEGREE OF
MASTER OF SCIENCE
IN
PHYSICS

By
Muhamet Ibrahimi
September 2019

LOGISTIC CELLULAR AUTOMATA
By Muhamet Ibrahimi
September 2019

We certify that we have read this thesis and that in our opinion it is fully adequate, in scope and in quality, as a thesis for the degree of Master of Science.

Oğuz Gülseren(Advisor)

Seymur Jahangirov

M. Cemal Yalabık

Mecit Yaman

Bekir Sıtkı Kandemir

Approved for the Graduate School of Engineering and Science:

Ezhan Karaşan
Director of the Graduate School

ABSTRACT

LOGISTIC CELLULAR AUTOMATA

Muhamet Ibrahimi
M.S. in Physics
Advisor: Oğuz Gülseren
September 2019

Cellular Automata (CA), initially formalized to investigate self-reproducing constructions, are among the most frequently used tools to model and understand complex systems. These computational frameworks are defined in discrete space-time-state domains, where time evolution occurs through local interactions. Despite the simple properties and the succinct absence of long range connections, these implementations have been proven proper for studying large scale collective behavior and self-organizing mechanisms which often emerge in dynamical systems. Following the spirit of the well-known Logistic Map, we introduce a single parameter that tunes the dynamics of totalistic CA by mapping their discrete state space into a Cantor set. By introducing this simple approach on two archetypal models, this study addresses further investigation of several complex phenomena: critical deterministic phase transitions, pattern formation and tunable emanation of self-organized morphologies in these discrete domains. We first apply this approach to Conway's Game of Life and observe sudden changes in asymptotic dynamics of the system accompanied by emergence of complex propagators. Incorporation of the new state space with system features is used to explain the critical points and formulate the tuning parameter range where the propagators adaptively survive, by investigating their autocatalytic local interactions. Similar behavior is present when the same recipe is applied to Rule 90, a totalistic elementary one-dimensional CA. In addition, the latter case shows that transitions between Wolfram's universality classes of CA can be achieved by tuning a single parameter continuously. Finally, we implement the same idea in other models and qualitatively report the expanding complexity that these frameworks support.

Keywords: Cellular Automata, Logistic Map, Game of Life, Rule 90, Critical Phenomena, Self-Organization.

ÖZET

LOJISTIK OTOMATIK HÜCRELER

Muhamet Ibrahimi
Fizik, Yüksek Lisans
Tez Danışmanı: Oğuz Gülseren
Eylül 2019

Başta kendini çoğaltan yapıları araştırmak için tanımlanan Otomatik Hücreler (OH), karmaşık sistemleri anlamakta ve biçimlendirmekte sıklıkla kullanılan aygıtlardandır. Bu bilgi-sayımsal yapılar, zamansal evrimin yerel etkileşimler yoluyla meydana geldiği ayrık uzay-zaman-durum alanlarda tanımlanır. Basit özelliklerine ve uzun erim bağlantılarının özlü yokluğuna rağmen, bu uygulamalar geniş çaplı toplu davranışlı ve kendi kendini organize eden ve sıklıkla dinamik sistemlerde ortaya çıkan mekanizmaların doğru araştırılmasında kendilerini ıspatlamışlardır. Tanınmış Lojistik Haritanın benzer şekilde, bütünsel OH-in ayrık durum uzayı bir Cantor kümesine döndürerek, bu sistemlerin dinamiğini ayarlayan tek bir değişken sunuyoruz. Bu basit yaklaşımı iki örnek model üzerine sunarak, bu çalışma bir sürü karmaşık olguların daha ileri araştırılmasını öne çıkarmaktadır: özellikle kritik deterministik faz geçişleri, desen oluşumu ve bu ayrık alandaki öz örgütlenen morfolojilerin ayarlanabilir ortaya çıkışı.Bu yaklaşımı ilk olarak Conway'in Hayat Oyununa uyguluyoruz ve karmaşık yayıcıların ortaya çıkmasıyla beraber sistemin asimptotik dinamiğinde ani değişiklikler gözlemledik. Yeni durum uzayın sistemin özelliklerine katılması: kritik geçis noktalarını açıklamak ve yayıcıların otokatalitik yerel etkileşim dizilerini araştırarak, dayandıkları ayar değişken aralığını formüle etmekte kullanılabilir. Bütünsel temel bir tek boyutlu OH olan Kural 90'a aynı tarif uygulandığında da benzer bir davranış mevcuttur. Ek olarak, ikincisindeki durum, OH sınıfları arasında deteministik geçişlerin tek değişkenin sürekli ayarlanmasıyla başarılabileceğinin bir göstergesidir. Son olarak, aynı fikri farklı modellerde uygulayabiliriz ve bu yapıların desteklediği genişleyen karmaşıklığı niteliksel olarak gösteriyoruz.

Anahtar sözcükler: Otomatik Hücreler, Lojistik Harita, Hayat Oyunu, Kural 90, Kritik Fenomenler, Öz Örgütlenme.

Acknowledgement

I would like to express my utmost gratitude to Prof. Oğuz Gülseren for his kind advisorship filled with help, support, and tolerance in every single moment of this study. I thank him for his trust and guidance while encouraging me to explore the field I loved most.

I would like to thank Dr. Ghaith Makey, Assist. Prof. Serim Ilday and Assoc. Prof. Ömer Ilday for "conceiving" within me an inexpressible affinity towards complexity science. Times of their guidance are the best I have had during my undergraduate years at Bilkent University. I also thank my instructors, Assoc. Prof. M. Özgür Oktel, Prof. Ceyhun Bulutay and Prof. M. Cemal Yalabık for being excellent models through their lectures and discussions.

I have felt deep encouragement and inspiration from my family: my mother Zamira; my brothers Ergest and Oltjon; and my sister-in-law Tommy Rose who brought to us an amazing little dragon, Oliver.

I thank my life comrades Xhon Lalo and Tedi Brahimi for sharing their worlds with me. I thank my graduate study mates Enes Aybar, Muhammed Bilgin, Umutcan Güler and Murod Bahovadinov for their warm companionship and fruitful discussions. I am also grateful to my friends Suard Cengu, Erta Xhafa, Fjola Hyseni, Redjon Xhepa and Kübra Yüksel for their close friendship, care and support.

Last but not least, I feel very privileged to have been chosen to work with Assoc. Prof. Seymur Jahangirov. I thank him for setting both of us free to dive into an endless sea of ideas and reflections, most of which are encapsulated in this study. His passion, creativity and conduct have affected every paragraph of this thesis, as well as my way of thinking.

Had we known what this was about
Had we noticed the time running out
We'd be louder than a thundercloud
Just for you, to make you proud...

To my father, Rushit.

Contents

List of Figures

Chapter 1

Introduction

1.1 The Beauty of a Discrete Realm

Cellular Automata (CA) , computational frameworks related to many fundamental fields of science, were first introduced by mathematicians, got developed with the rise of computer science, and then found applications in fields such as physics, chemistry, biology, ecology and social sciences. When discussing the origins of the field, scientists usually refer to A. Turing, J. von Neumann, S. Ulam, J.H. Conway, S. Wolfram as pioneers with important contributions in development of the field.

The first person who came with a formal definition of CA is John von Neuman [1]. The question he addressed was about the minimal conditions of a structure with internal capacities of generating replicas of itself, that is, self-reproduction. At this point, a biologist would think that this idea addresses the fundamental conditions for biological inheritance, whereas a computer scientist would think of a practical robot that, among many different tasks, is able to create another identical copy of itself. Not surprisingly, in the following years people would consider these frameworks as paradigms of self-organizing systems and would also start developing ideas on artificial life [2].

Von Neumann introduced a structure that could on its own generate a replica of itself that inherits the same properties of its progenitor. He defined specific settings: a space tessellated in identical units (agents) arranged in a lattice, time operating in discrete steps, and a finite number of states that were to assign certain "kinds" or functionalities to the agents. More importantly, the key idea is that the evolution of the system was designed to be internally driven by local parallel rules that apply to each agent, rather than being controlled by a central unit [1].

This idea suggested a bottom-up approach of modeling and understanding the macro-scale behavior in a plethora of real systems. The literature nowadays presents CA as phenomenological tools to study pattern formation, self-organization and collective behavior in areas of physics [3], chemistry [4], biology, ecology, geology [5], economy, and urban [6] or social [7] systems. A couple of examples might include fluid flows [8], Ising models [9], nucleation-aggregation and crystal growth [10] , reaction-diffusion systems, cell migration, tissue development, or epidemics spreading models [11, 12, 13]. Moreover, out of the rich spectrum of behavior that CA can generate, it has been essential in fundamental development of several fields such as self-organized criticality [14], percolation theory, dynamical systems theory, computer and complexity science [15].

Next to von Neumann, Stephen Wolfram is another important contributor who studied the fundamentals and applications of CA, based on very simplistic one dimensional models. He suggested a classification map for such systems, showing qualitatively four statistical types of behavior (discussed below) [16]. Next, several contributors like Codd, Langton, Toffoli have helped to expand the understanding of such systems and also suggesting applications of CA as tools for modeling real systems. They were part of the first scientists to realize the role of CA among different tools of study. Actually, CA have also been considered not just as approximate schemes, but appropriate environments [17, 18] for modeling physical systems. Our perception of a continuous space, time and states, is often modeled via integro-differential systems of equations. However, the tendency to simplify the tools of study is a common philosophy in science. In a simpler level, a dynamical system with discrete space is modeled via coupled ordinary differential

equations. Further simplification by discretizing the time, but keeping the state space as continuum, brings up the so called finite difference systems and coupled map lattices. The most reduced version, which is discrete in every term, is nowadays known as a cellular automaton. Compared to classical tools of dynamical systems theory and statistical mechanics, CA have proven to be more effective in modeling complex dynamical systems of order and disorder, where large scale collective behavior and self-organization appear. Central limit theorems apply only in systems in thermodynamic equilibrium, and dynamical processes of large numbers of components (variables) are far out of the scope of the limited dimensional phase portraits offered by dynamical systems theory [15]. In turn, CA models can provide the underlying multi-component nonlinear interactions in complex systems, which often operate out of equilibrium. The difference lies in applying parallel local interactions to each agent in the system.

Covering a broad scope, CA are also classified in several types, depending on their properties of time evolution. The time evolution initially was applied in a purely deterministic fashion but at some point, models where random components were introduced, became popular. Probabilistic CA, in which there is an associated probability to each rule of operation, are an important group that have increased the applicability of these systems. At the same time there are systems where the sites updating scheme is not simultaneous, thus introducing the type of asynchronously updated CA. Given the neighborhood structure and the state space, it is straightforward to calculate the number of possible rules of a model. Usually even minimal conditions provide a considerable number of local interactions that generate several nonlinear and complex phenomena [16]. Another type is the so called totalistic CA, accounting for a specific group of interaction rules in which the state of a site depends on the total (sum) of its neighboring states, thereby introducing some kind of "isotropy" in the system. On the other hand, lattice gas (LG) CA are models widely used in fluid physics and biology, and are often considered as microscopic approaches for fundamental understanding of relevant phenomena. Namely, the famous HPP model [8] is an automaton that in macro-scale generates the same behavior with the Navier-Stokes system of equations in certain settings. There is also a CA type in which the state space

is a probability density, instead of a discrete set. Such systems are called lattice Boltzmann (LB) models and are also used for mimicking physical and chemical systems [11].

The extension presented in this thesis applies to the group of two-state totalistic CA. Motivation of this study lies on the vision of exploring even more phenomena in the spectrum of CA, more specifically related to phase transitions, pattern formation and self-organization in the complex systems. It is a common philosophy of research to explore the frameworks by slightly deviating from the basic definitions, as Chopard suggests: "... it is acceptable (and even beneficial) to relax some of the constraints of the original definition of a cellular automata... The point is to conserve the spirit of the approach and its relevant features rather than its limitations." [19] Our idea lies in introducing a parameter that alters the dynamics of these frameworks by tuning the rate of change of the states. This intervention preserves the deterministic nature of systems (if the rules are so) and can be applied to many models to suggest new phenomenological examples of complex behavior, yet with the cost of state space expansion.

1.2 Organization of the Thesis

In the introduction we present a set of definitions that narrowly applies to the two-state of totalistic CA, systems with boolean states and local rules in which the state of each agent depends only on the total (sum) of it's neighborhood states. We present only the lattice geometries and types of neighborhoods considered in this thesis, however, the reader can refer to the following ref. [12, 15, 19] for the most general definitions. Introduction also contains brief descriptions of two famous totalistic CA, which are also the main target platforms of the study, Conway's Game of Life (GoL) and Wolfram's Rule 90.

Chapter 2 presents a brief introduction of the Logistic Map, as our inspiration for implementing a single parameter to achieve transitions in dynamical systems. We rewrite Conway's Game of Life rules in a finite difference form in order to

implement the tuning parameter. Then we analyze its effects on the state space, which turns out to expand into a Cantor set. Lastly, we introduce the definition of operations, which arise from the finite difference form interpretation of local rules, and turn out helpful for quantitative analyses in the later chapters.

Chapter 3 includes a series of numerical and analytical analyses related to the asymptotic dynamics of Game of Life. We report mean field results which predict the asymptotic density. Next, we observe a series of transitions in the order parameter and try to incorporate the new state space with properties of the framework to explain the source of these transitions. The framework which introduces the Logistic GoL defines two main regimes, a sparse inactive phase (in the same universality with Conway' GoL) and a dense active phase which is subject to pattern formation as the parameter is tuned. To quantitatively observe the parameter dependent dynamics of pattern formation, we introduce a neighborhood correlation function.

In Chapter 4 we report observations of an unprecedented nature. We discuss how a single parameter can not only introduce a global change in dynamics and lead to pattern formation, but also influence on smaller scale self-organization of spatio-temporal correlations, often referred to as propagators (spaceships) and replicators. We initially discuss the notion of these coupled interaction sets and how they apply to the Glider in Conway's GoL. Then we pay special emphasis on a propagator whose stages do not fully exist in Conway's GoL but build up step by step as the parameter is tuned, and it turns into a powerful attractor inside its operation range. Then we briefly present other instances of self-organization that appear in different ranges of the parameter.

Chapter 5 includes a detailed analysis of the logistic extension on Wolfram's Rule 90. We present how the extension applies to this automaton and show that the influence of the same parameter provides results similar with the ones observed in the Logistic GoL. We report a series of changes that make the automaton subject to a transition within the universality classes defined by Wolfram. Besides the emergence of a propagator in one dimensional settings, we also observe how the tuning of parameter enables the transformation of this structure

into another, more complex propagator.

In Chapter 6 we report very brief and qualitative results of this extension to other totalistic CA models, showing how a tuning parameter can expand the range of complexity that each framework can explore. Rules adapted from Larger than Life, Majority (Growth) model, and Life-Like CA are discussed along with an outlook on the whole study.

1.3 Archetypal Models

In this section we present a set of definitions specifically referring to totalistic CA, which is the target group of this study. Moreover, we introduce two important models that have been extensively studied in the literature. The same systems are going to be studied in detail throughout the thesis.

1.3.1 Definitions

The definitions presented here are not applicable to the most general formalism of CA, but rather focused on a certain group. Initially define some "physical grounds" where the dynamics occur, and in this field it is commonly referred to as cellular space. It is usually a regular lattice (providing uniformity for each unit) and can in principle be of any dimension. Most of the introduced models are in one (1D) and two (2D) dimensional settings. In 2D the cellular space is often chosen to be a square or hexagonal lattice. The space and time are discrete hence there is no need for specifying any units. Each site $s(\mathbf{r}, t)$ is assigned one of the available states determined by the modeler when designing the framework. Here we restrict our study to systems with two available states, which can be assigned by "dual" elements of a group, (populated/empty, spin up/down, dead/alive). Hence, we initially define a binary state space ($\tilde{\mathbf{S}} = \{0, 1\}$). Each site is to evolve within the states present in $\tilde{\mathbf{S}}$ according to local rules, by definition. Rules are also determined by the modeler. The usual approach is that the state of a site at

the upcoming time step depends on a set of rules based at the previous time step only. However, there are also CA with memory where the state depends on some of the previous time steps, but this is beyond the scope of our study. Since the rules are locally operating, the modeler has to define a neighborhood range, and since the lattice is uniform, the neighborhood will be the same for each site. In rectangular coordinates, it is common to define a radius ϕ, of the neighborhood coordinate set $N(\mathbf{r}, \phi)$ covering a total (rectangular shaped) range of $(2\phi + 1)^D$ cells. D accounts for the dimensionality of the cellular space. The sum of the states in a neighborhood is thus:

$$m(\mathbf{r}, t) = \sum_{\mathbf{r'} \in N(\mathbf{r}, \phi)} s(\mathbf{r'}, t)$$

Once the neighborhood sum m is computed, every site goes through a simultaneous (parallel) updating scheme:

$$s(\mathbf{r}, t + 1) = s(\mathbf{r}, t) + \Delta s$$
$$\Delta s = \mathbf{R}(m, s)$$

This way, the iteration update $s(\mathbf{r}, t) \rightarrow s(\mathbf{r}, t + 1)$ carries on at every site and time step. The change in each site Δs, is a function with a range within the set of rules $\tilde{\mathbf{R}}$, and depends on m and s. This scheme is usually represented by a rule table that shows how states change given the possible neighborhood sums. When defining the neighborhood sum m, it is important whether the central site s is included in the sum or not. If s is not included in the neighborhood then the automaton is called outer totalistic, and this is the case for both Conway's GoL and Wolfram's Rule 90. Note that there are also asynchronous updating schemes, where sites at each time step are given a probability of updating, but this is also beyond the scope of this study.

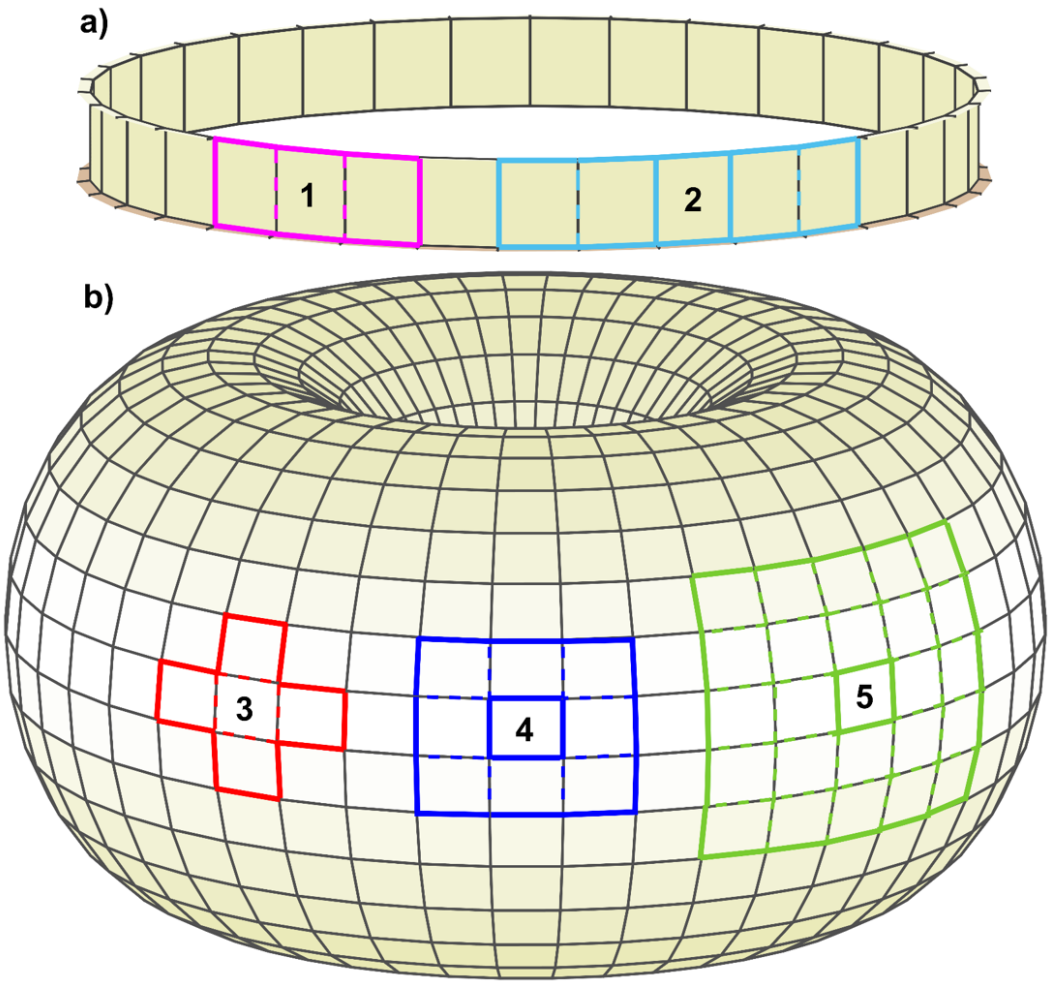

Figure 1.1: (a) One dimensional cellular space with periodic boundary conditions. 1 and 2 represent two different neighborhoods of $D = 1$, $\phi = 1$ and $\phi = 2$, respectively .(b) Two dimensional cellular space of square lattice and periodic boundary conditions. 3 represents the von Neumann neighborhood, 4 ($D = 2$, $\phi = 1$) is the Moore neighborhood and 5 is an example of larger neighborhoods ($D = 2$, $\phi = 2$).

Another important element of these systems is deciding the boundary conditions, which may have crucial effects depending on the system. Every model in this study is simulated under periodic boundary conditions. A 1D cellular space is folded in the shape of a ring and the 2D space has a torus as its counterpart, shown in Fig. 1.1. A last note needs to be done on the neighborhood geometries, which depend on the dimensions and symmetry of the cellular space. We are going to consider systems mostly with axial neighborhoods in quadratic coordinates.

In 1D , a $\phi = 1$ represents a neighborhood with the central site and two nearest neighbors. In 2D, the smallest symmetric neighborhood is the so called von Neumann neighborhood (what von Neumann used in his automaton), whereas a $\phi = 1$ in 2D represents 8 nearest neighbors, also known as Moore neighborhood. Not surprisingly, the cases 1 and 4 in Fig. 1.1 are the neighborhoods defined in Wolfram's Rule 90 and Conway's GoL, respectively.

1.3.2 Game of Life

In 1970's the mathematician John H. Conway introduced an CA model to show that simple rules can lead to very complex behavior, and Game of Life (GoL) turned out the most famous and most studied automaton. It is an outer totalistic model of simple rules, defined in a two-dimensional square grid of cells and designed with two states, referred to as dead and alive respectively. Each time step is referred to as a generation in the system, and every site is updated synchronously via the following rules. Any live site with fewer than two or more than three live sites in its Moore neighborhood will decay (die) in the upcoming generation. A dead site needs to have exactly three living neighbors to grow (become alive) in the next generation. And the live sites will remain so in the upcoming step only if they have two or three live neighbors.

These simple settings surprisingly provide very complex dynamics that stabilizes with a long transient time. An observation of cellular space shows how sites interact to generate a large set of stable, oscillating and propagating structures as the system evolves from random initial conditions. A series of snapshots is presented in Fig. 1.2 to illustrate the dynamics and activity of these interactions. Activity in Conway's GoL is nonlinear, it might get localized in certain regions but also spread in larger parts of the domain as the system evolves through time [20]. Albeit being simple and not really related to any physical system, Conway's GoL has always been considered as a powerful dynamic framework to understand complexity and emergence.

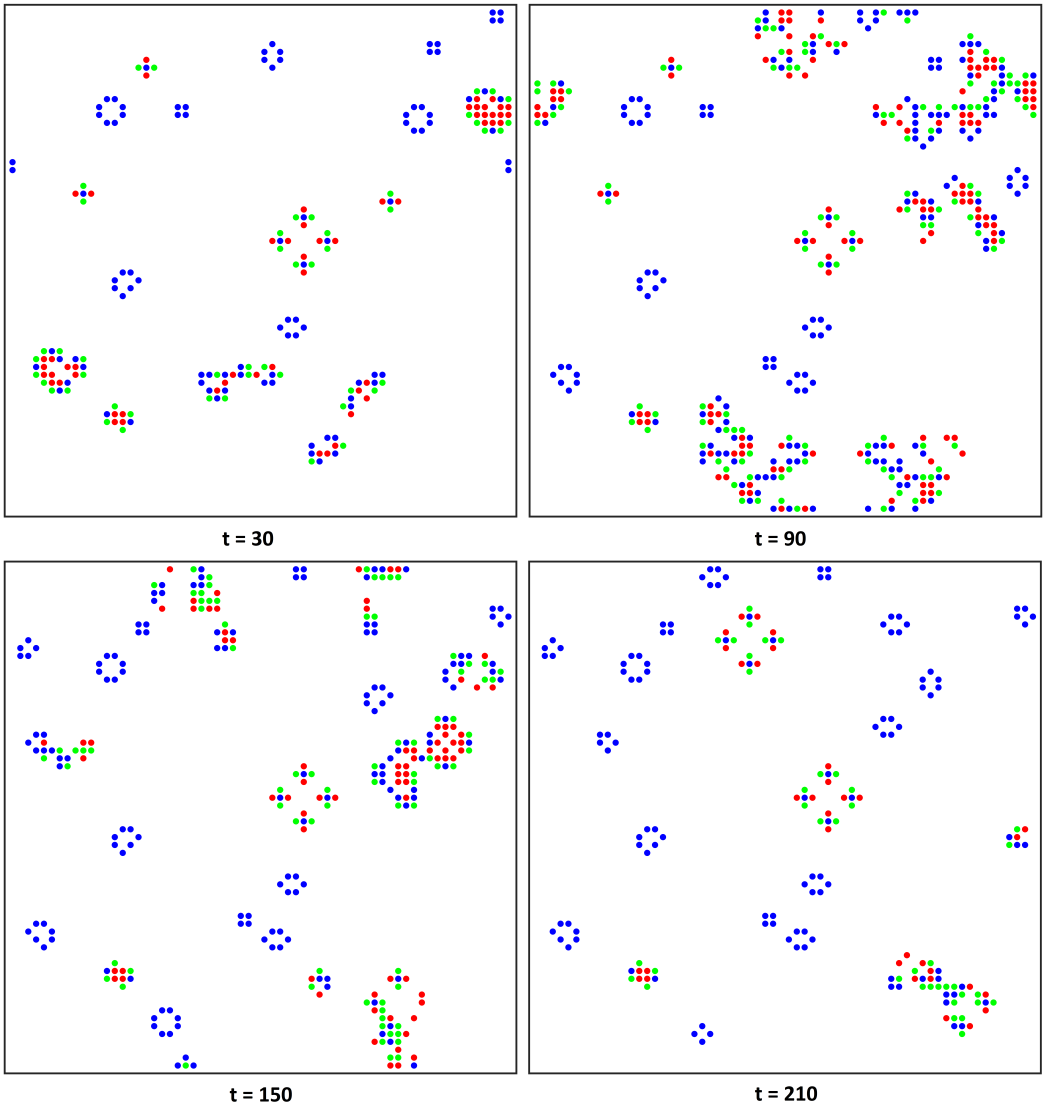

Figure 1.2: Conway's Game of Life set from random initial conditions with a density $\rho_0 = 0.5$. (●) are live sites which remain stable, (●) are dead sites which grow, and (●) are live sites which decay in the following time step.

Asymptotic density and time evolution in GoL have been analyzed in detail by earlier theoretical approaches. The first implementations reported on this system are mean field theory and a statistical model based on GoL [21]. Later on, Bagnoli et. al provided a more thorough analysis on the mean field analyses and reported interesting results regarding the activity and time evolution [22]. Generalizations of GoL include deterministic systems with variations in the rules, where other totalisic CA were explored in terms of dynamics, patterns and time

evolution [23, 24]. Within this group, GoL rules are known to generate an inactive asymptotic and subcritical behavior and with a long transient time, features making this system as a target tool for more investigation. Further studies, still within the deterministic rule domain, include expansion in the neighborhood by introducing the family of Larger than Life (LtL) [25]. Larger neighborhood induces an exponentially higher degree in complexity and this is clearly observed in the enormous variety of structures and patterns presented in the studies of LtL.

Another interesting approach regarding the neighborhhod expansion is introduced by Huang et. al, where a non-local connectivity [26] between sites induces second-order transitions in activity and density [27]. In turn, transforming GoL into a probabilistic CA also introduces critical transitions in density [28]. Furthermore, critical phenomena are observed even when the synchronicity in GoL is broken by tuning the updating scheme to an asynchronous Poisson limit [29]. These generalizations are accompanied by additional tunable parameters and conclude that GoL is a subcritical system dominated by quiescent states but the same framework is yet associated with critical transitions in its dynamics. Same conclusion is reached when GoL is compared to the so called set of Life-Like CA [30]. Scale-free properties of GoL have also been investigated in the context of self-organized criticality where the system is subject to slight external perturbations [31]. Recently, there were suggested GoL like models in different lattice geometries [32] and also in 3D cellular spaces [33].

1.3.3 Rule 90

Stephen Wolfram is one of the early pioneers of the field and, among many contributions, he is also known for introducing the family of 1D elementary CA [34]. Frameworks modelled in minimal settings: a 1D cellular space, binary state space and the smallest possible neighborhood of $\phi = 1$. It consists of a total of 3 cells, as shown in Fig. 1.1(a). In total, there are 2^{2^3} possible combinations of the binary arrangements in this case, hence 256 possible rules that these settings can offer.

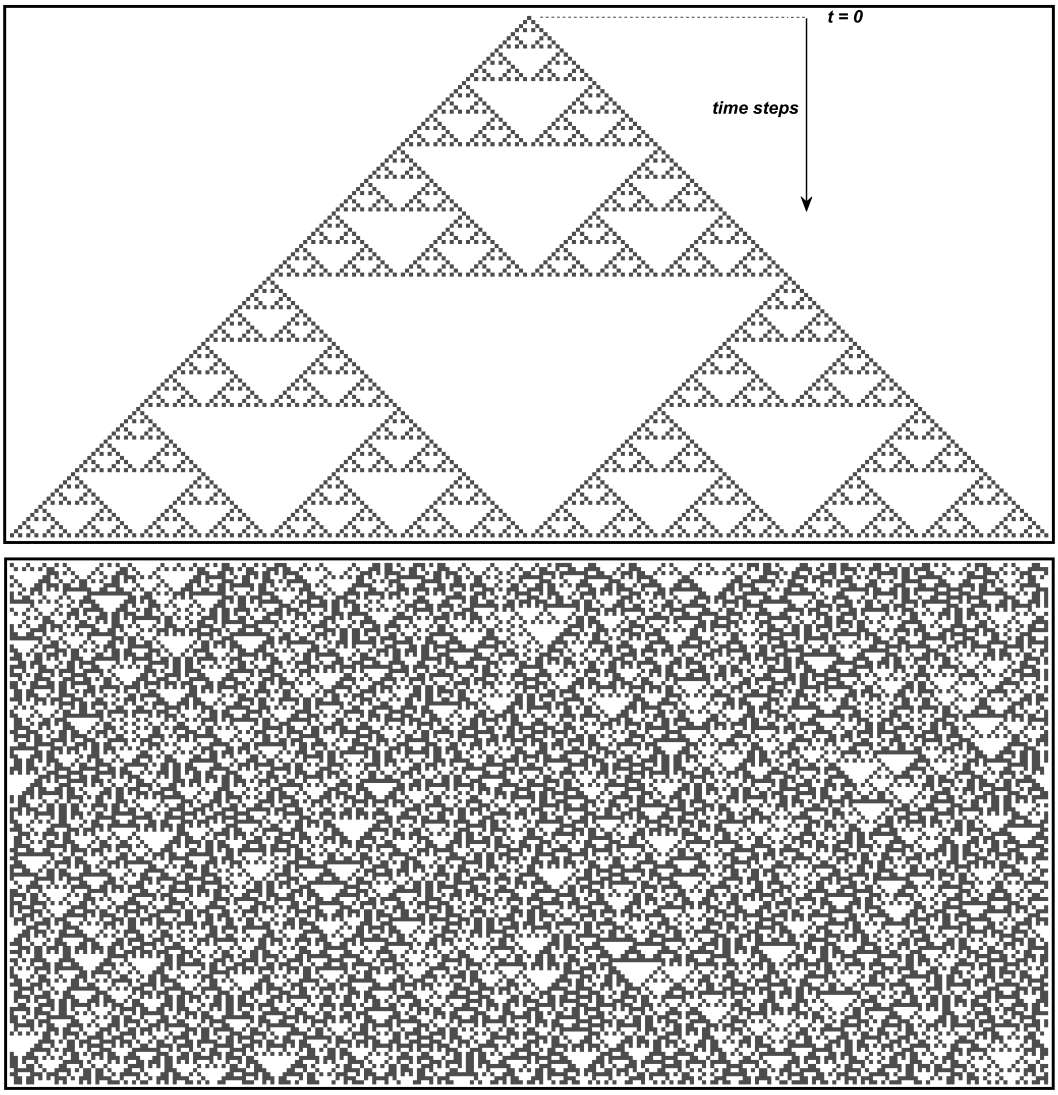

Figure 1.3: Wolfram's Rule 90 starting with a single live cell to generate Sierpinski triangle as the system evolves (above) and its chaotic behavior when starting from random initial binary distribution of initial density $\rho_0 = 0.25$ (below).

Each rule is named after a number according to Wolfram's binary scheme. It is important to mention that Wolfram presented a qualitative CA classification scheme for these rules, that in principle could be used to classify every other CA model according to its corresponding asymptotic dynamics. We are going to discuss this classification briefly as it is a useful prerequisite for Chapter 5.

Most of CA rules turn out to be dynamically irreversible, that is, a certain asymptotic configuration can be achieved through different initial conditions.

This is a key factor that encourages one to run different CA from random initial conditions and obtain a general classification for each of the rules. The classification according to Wolfram pools CA in four different groups, often called universality classes. Class I include systems in which random initial conditions eventually converge to a homogeneous phase, with all sites ending up in the same state. Class II groups the systems in which the rules end up generating simple stable or periodic oscillatiory states, what we call inactive asymptotic states. Class III refers to systems that produce a chaotic behavior and Class IV are systems that, among stable or periodic states, generate complex localized structures, periodically propagating throughout the lattice.

Rule 90 is the "parity" rule of the family of elementary CA. The central site becomes or remains populated in the next generation if there is only one populated site in its neighborhood. Having both or none of the neighbors populated, yields decay to the site in the following time step. What makes this rule famous is the time-space diagram when the system is set from a single populated site, generating the fractal structure of Sierpinski triangle as shown in Fig. 1.3. Rule 90 is a Class III automaton, producing chaotic behavior, yet features of self-organization [35] are present in the correlations between sites which form triangular voids (see Fig. 1.3).

Chapter 2

The Logistic Game of Life

2.1 The Model

2.1.1 Logistic Map

In 1976 Robert May introduced a simple iterated equation of a single variable updated in discrete time domain [36]. These equations are nowadays simply known as maps. Strogatz provides a useful related chapter with an intuitive analysis on the famous Logistic Map, considering maps as proper tools for studying differential equations, models of natural phenomena and chaotic transitions [37]. These abstract models consist of a simple tuning parameter which affect the dynamics of the system. The Logistic Map is thus the iterated equation of a population $\mathbf{x}$:

$$\mathbf{x}_{t+1} = r\mathbf{x}_t(1 - \mathbf{x}_t)$$

The steady state solution of the system exhibits enormous changes under the influence of parameter r. Initially it converges to a single attracting point that changes as the parameter is tuned, but at some critical point the system becomes bistable and $\mathbf{x}$ oscillates between two different values. This period doubling is

repeated indefinitely until the system hits chaos, namely becomes aperiodic. The effect of tuning parameter is shown in Fig. 2.1. The critical values where period doubling occur were studied by Feigenbaum, who used renormalization techniques to come up with a ratio that is equivalent for a larger family of equations, the so called unimodal maps [37]. The implementation of a parameter in simple iterated variables is the main inspiration of our study. We manage to rewrite Conway's GoL rules in a finite difference form and then apply a tuning parameter in a similar fashion.

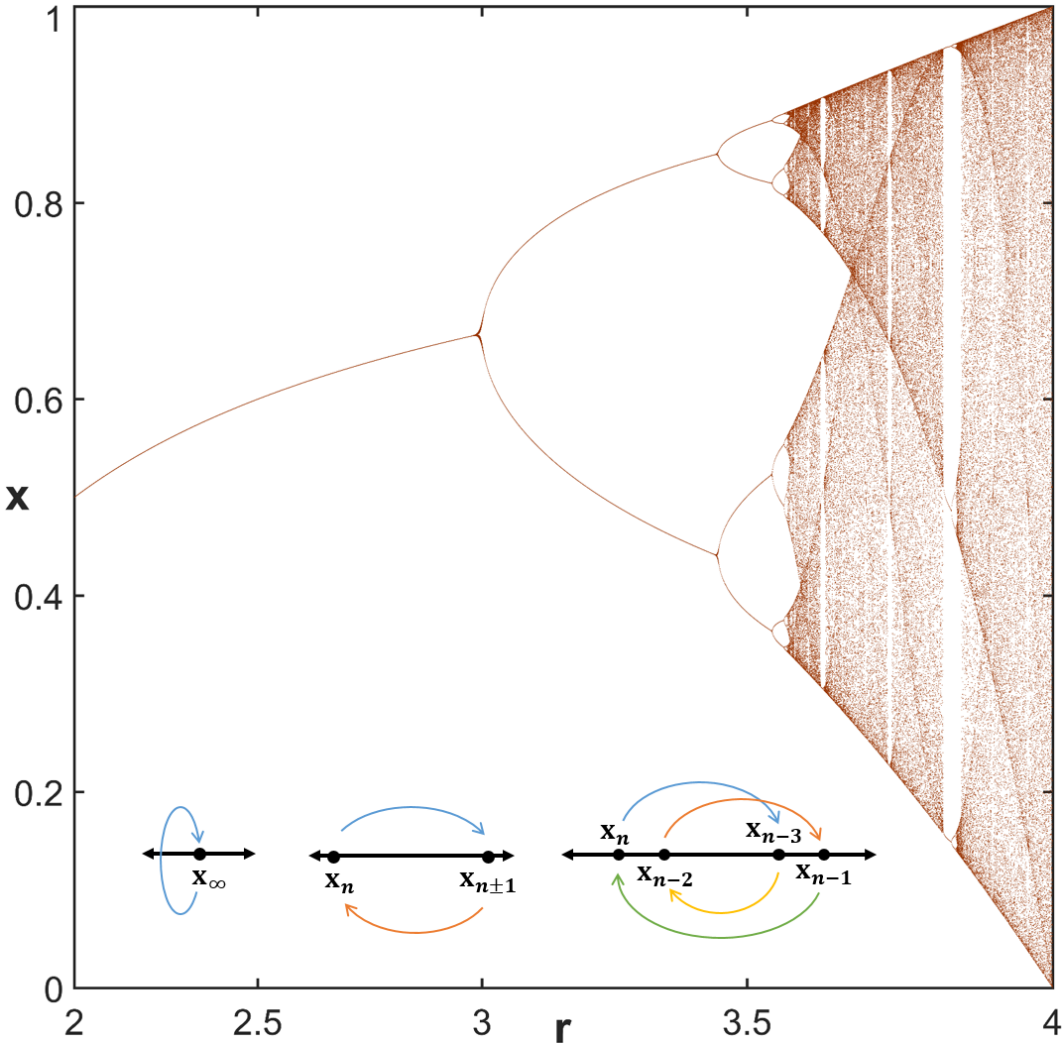

Figure 2.1: Population **x** versus tuning parameter r in the Logistic Map. From a single steady state solution the system reaches chaotic behavior after a series of period doubling bifurcations. Illustrative diagrams are shown in the bottom.

2.1.2 Rewriting the rules in Game of Life

In Conway's GoL the state of a cell, s, is synchronously updated according to the sum of states m in its Moore neighborhood, as shown in Fig. 2.2(a). The change in a state, Δs, can be defined by the rate equations that comply three regimes: decay, stability and growth, offering a clear picture of the non-equilibrium conditions present in the system. If $m < 2$ or $m > 3$ then $\Delta s = -s$ which in a two-state system indicates asymptotic decay. $m = 2$ corresponds to stability, hence $\Delta s = 0$. Finally, if $m = 3$, then $\Delta s = 1 - s$ indicating asymptotic growth.

We extend GoL by introducing a single tuning parameter λ that re-scales the updating rate, with $\lambda = 1$ corresponding to the original system. Actually these update equations are the same with the first order finite difference forms of exponential decay and asymptotic growth equations, respectively (see table in Fig. 2.2). In the new system, sites are still subject to three possible rules, but with several consequences in the state space $\tilde{\mathbf{S}}$. We denote the updating rules as decay (D), stability (S) and growth (G) operations:

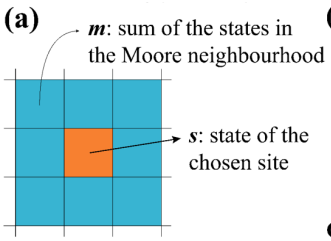

(b)

	Conway's Game of Life		Logistic Game of Life	
	Condition	Δs	Condition	Δs
Decay	$m = 0, 1, 4, 5, 6, 7, 8$	$-s$	$m < t_1 \vee m > t_3$	$-\lambda s$
Stability	$m = 2$	0	$t_1 \leq m < t_2$	0
Growth	$m = 3$	$1-s$	$t_2 \leq m \leq t_3$	$\lambda(1-s)$
Operation Regions	0 1 2 3 4 5 6 7 8		0 t_1 t_2 t_3 8	

Figure 2.2: Central site at state s determined by the sum m of the eight states in its Moore neighborhood ($\phi = 1, D = 2$) . The table shows the three operation regimes: decay, stability and growth. In the case of Logistic GoL, the difference equations are re-scaled by the parameter λ. Operation regions are discrete in Conway's GoL while in Logistic GoL they are continuous domains separated by parameters t_1, t_2 and t_3.

$$\mathbf{D}s \Rightarrow (1-\lambda)s$$
$$\mathbf{S}s \Rightarrow s$$
$$\mathbf{G}s \Rightarrow (1-\lambda)s + \lambda$$

At this point, the rule set is actually transformed into a set of operations, $\tilde{\mathbf{R}} = \{\mathbf{D}, \mathbf{S}, \mathbf{G}\}$. This perspective is an essential transformation that needs to be followed if our framework is to be implemented into another automaton. It will become obvious that interesting transitions and dynamics can be achieved only if the systems are totalistic. In turn, operations are an alternative approach to numerical results for gaining a better understanding on the system. We will observe that recording the operations at each site can provide a polynomial representation of the states, which serves as an analytical tool for analysis of emergent phenomena.

2.2 State Space Expansion

2.2.1 Cantor Set

For the range $0 < \lambda < 1$, $\tilde{\mathbf{S}}$ is eventually transformed into a Cantor set within the range [0,1]. The formation of this λ-dependent Cantor set is schematically shown in Fig. 2.3. If one starts with a continuous set between 0 and 1, the decay and the growth operations will map these values to shrunk intervals with limits $[0,1-\lambda]$ and $[\lambda,1]$, respectively. Here both decay and growth operations map the states and increase the distribution density only within these smaller regions while stability operation has no such effect. After the first iteration, the range $[1-\lambda,\lambda]$ is still populated by values remaining the same due to stability operation. However, they keep fading with subsequent iterations (sites which experience only stability in randomly initialized runs are statistically very rare), and hence are not shown. The boundary values $\{0, 1-\lambda, \lambda, 1\}$ formed after the first iteration are named as first order elements of the Cantor set. Upon the second iteration,

these boundaries are preserved while new boundaries are formed by addition or subtraction of $(1-\lambda)^2$, leading to $\{(1-\lambda)^2, 1-\lambda-(1-\lambda)^2, \lambda+(1-\lambda)^2, 1-(1-\lambda)^2\}$.

Preserved and new boundaries together make up the second order elements of Cantor set. After n iterations one reaches at n^{th} order Cantor set elements, 2^{n+1} unique values which are spaced in a self-similar fashion in the range [0,1]. Every element of n^{th} order Cantor set can be written as a sum $c_0 + c_1(1-\lambda)^1 + ... + c_{n-1}(1-\lambda)^{n-1} + c_n(1-\lambda)^n$ with proper coefficients that take values -1, 0 or 1. Our preferred way of representing elements of the Cantor set is to write them as series of decay and/or growth operated on 0 or 1. As seen in Fig. 2.3, the order of polynomial representing a state is equal to the total number of decay and growth operations involved.

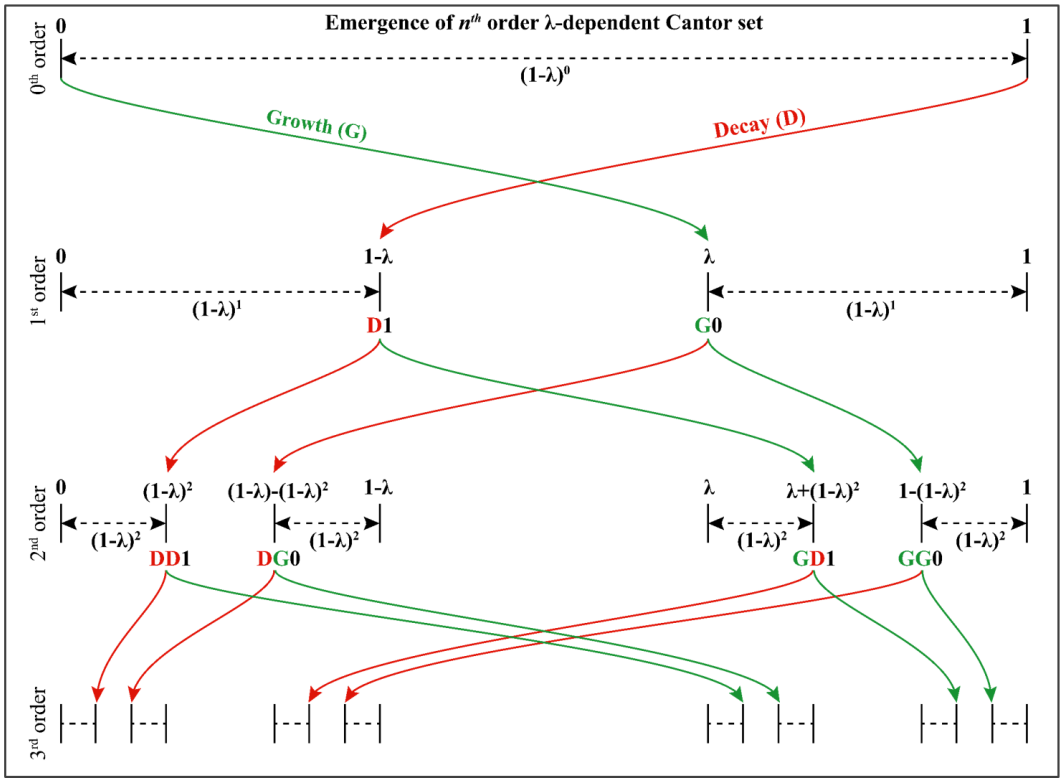

Figure 2.3: An initially continuous distribution gets shrunk in narrow regions as the operations act on the values, and an indefinite iterative application of operations yields an infinite set of zero length, known also as Cantor set.

With the new state space we need to consider its effects on the neighborhood space $\tilde{\mathbf{M}}$, which in turn dictates the rules. Now $\tilde{\mathbf{M}}$ spans the range [0,8] populated by eight-fold convolution of the Cantor set. To account for this, we fairly assign two unity intervals centered at 2 and 3 as stability and growth regimes, respectively, with the rest corresponding to decay. The limits of these intervals are represented by $t_1 = 1.5$, $t_2 = 2.5$ and $t_3 = 3.5$, as shown in Fig. 2.2. The new automaton is named Logistic GoL and it is still synchronous, outer totalistic, discrete in space and time but now with an extended state-space. Thus, in terms of classification, it can also be regarded as a coupled map lattice [38, 39].

2.2.2 Numerical Investigations

To further clarify how the Cantor set emerges in Logistic GoL we perform actual simulations of the Logistic GoL in a 1000×1000 square lattice with periodic boundary conditions. Initially the states in each cell are picked up randomly from a uniform distribution in the range [0,1]. We start 3000 unique runs with different λs linearly spanning the range (0,1]. After a certain number of iterations, we take a histogram that counts the number of occurrences of values that falls into one of the 1000 bins that uniformly parses the state domain between 0 and 1. The same is repeated 28 times with different initial conditions and the histograms are summed over the repetitions. Finally, we take the logarithm of the number of occurrences after increasing each by one (to avoid zeros). The resulting values depending on λ and s are represented with a color code (that spans from 0 to an arbitrary maximum) in a two-dimensional plot. Top panels of Fig. 2.4 shows this analysis for steps 1, 2, 3 and 1000.

One can clearly see the emergence of the first, second and third order Cantor set manifested as λ-depended boundaries highlighted with dashed lines. After 1000 iterations these boundaries remain while the regions in between fade away as described above. The bottom panels of Fig. 2.4 present the density of states for $\lambda = 0.8$. Here the lack of the logarithmic scale further establishes the contrast between high and low density regions separated by the Cantor set.

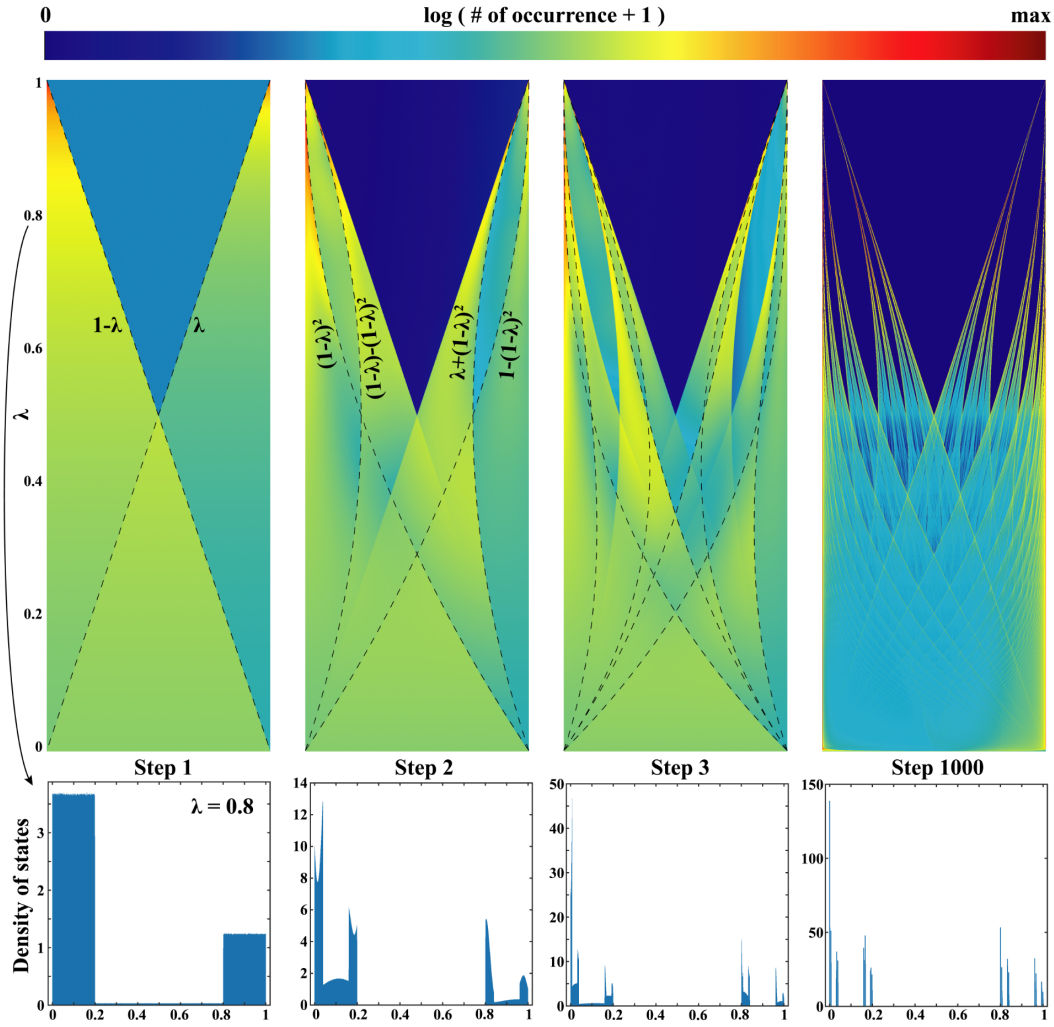

Figure 2.4: Top panels: the logarithmic distribution of states after 1, 2, 3 and 1000 iterations. Two-dimensional histograms of states are constructed for values of λ in the range (0,1]. The colors represent the logarithm of the number of occurrences plus unity, to avoid zeros (see text). Dashed lines correspond to Cantor set elements formed after corresponding iteration. Bottom panels: the density of states after 1, 2, 3 and 1000 iterations for $\lambda = 0.8$.

Chapter 3

Asymptotic Dynamics of the Logistic GoL

3.1 Mean Field

Studies that perform statistical analysis in CA often choose the density as the order parameter. We apply a single site mean field approach to the Logistic GoL in a similar fashion with earlier approaches [22, 21, 30], considering an initial density ρ_0 with a uniform probability distribution function $P(x)$ spanning a continuous range in [0,1]. Thus, for any ρ_0:

$$P(x) = \begin{cases} \frac{1}{b-a} & , \ a \leq x \leq b \\ 0 & , \ otherwise \end{cases} \tag{3.1}$$

$$a = max(0 \ , \ 2\rho_0 - 1); \quad b = min(1 \ , \ 2\rho_0)$$

so that $\int xP(x)\,dx = \rho_0$ and $\int P(x)\,dx = 1$ are accordingly satisfied. In turn, for an initial density ρ_0, the probability distribution of the Moore neighborhood sums, $P^{'}(y)$, becomes the eight-fold convolution of $P(x)$. Exploiting the convolution theorem:

$$P^{'}(y) = \frac{1}{2\pi} \int_{-\infty}^{+\infty} [p(f)]^8 e^{2i\pi yf} df \tag{3.2}$$

where $p(f) = \int P(x)e^{-2i\pi fx}dx$ is the Fourier Transform of $P(x)$. $P^{'}(y)$ is in fact a piece-wise function of eight different 7th order polynomials. Automaton's rules can be applied to probe the updated density ρ based on the general equation reconstructed from the rewritten rules in Figure 2.2(b) in Sec. 2.2:

$$\rho = \rho_0 + \lambda(k - \rho_0), \qquad k = \begin{cases} 0 & , \ P^{'}(y) < t_1 \ , \ P^{'}(y) > t_3 \\ \rho_0 & , \ t_1 \leq P^{'}(y) < t_2 \\ 1 & , \ t_2 \leq P^{'}(y) \leq t_3 \end{cases} \tag{3.3}$$

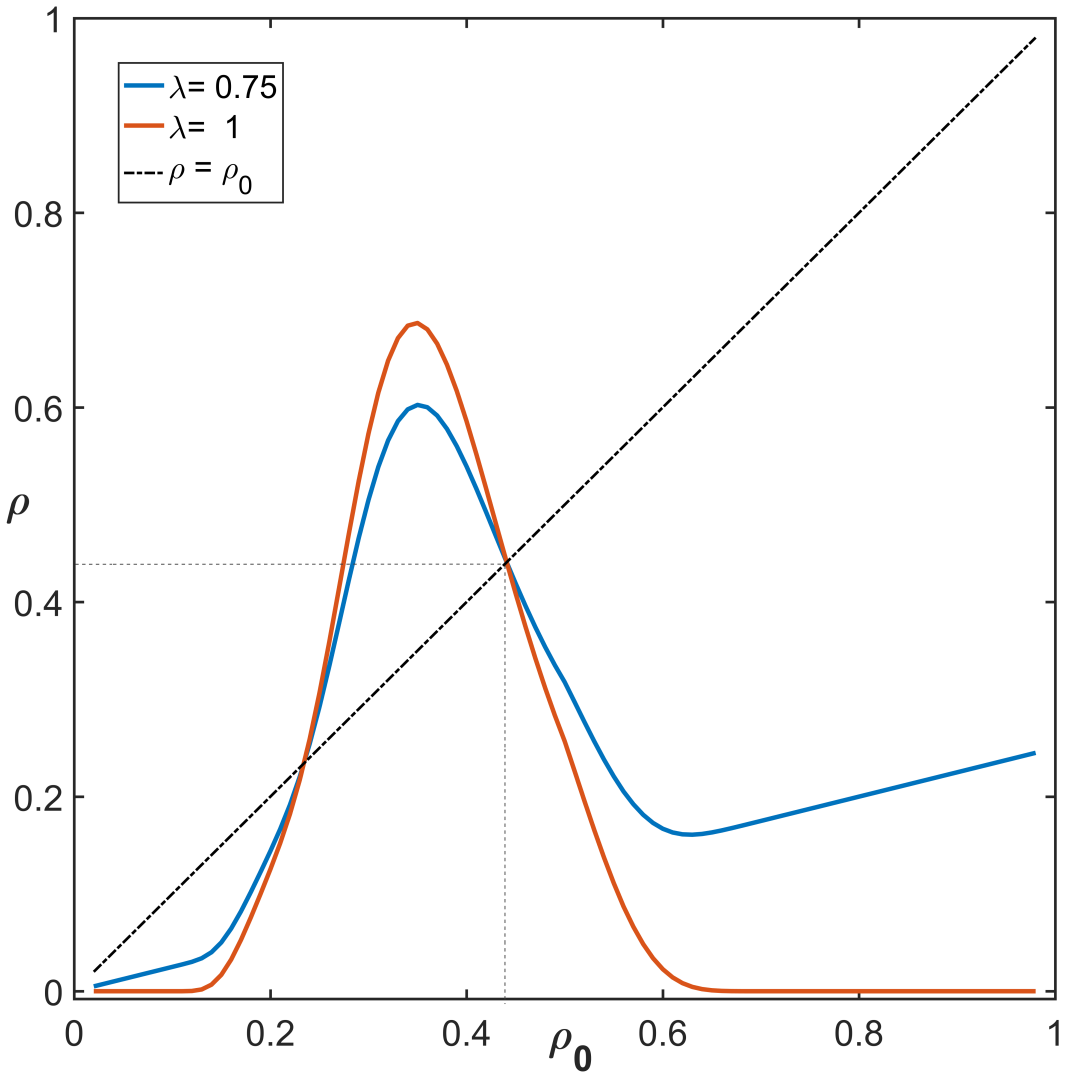

Figure 3.1: Updated density ρ vs. initial density ρ_0 of continuous uniform distribution, calculated using eq. 4 for $\lambda = 0.75$ (blue) and $\lambda = 1$ (orange) values.

Implementing $P^{'}(y)$ in the mean field equation eventually yields:

$$\rho = \rho_0 + \lambda \left\{ \rho_0 \left[\int_{t_1}^{t_2} P^{'}(y)\, dy - 1 \right] + \int_{t_2}^{t_3} P^{'}(y)\, dy \right\} \tag{3.4}$$

The updated density shown in Fig. 3.1 can be considered as a one-dimensional flow with two fixed points, the stable one being at $\rho \approx 0.4484$. The presence of λ is rather symbolic in this case, having no effect on the location of fixed points but only on the rate of the flow. An effective implementation of λ-dependent fixed points can be achieved by performing an iterated updating on the initial distribution function itself. However, the value obtained by these calculations turns out to be quite similar with numerical results presented in the next section.

3.2 Deterministic Phase Transitions

In this section we report numerical analysis of the Logistic GoL. Starting with $\lambda = 1$ and tuning it down, we observe changes in the behavior of the system as it departs from Conway's GoL. In accordance with previous studies on GoL, we choose the asymptotic density, ρ, as our order parameter. To calculate ρ, we start with a 1000×1000 square lattice with periodic boundary conditions. Initially the states are picked up randomly from a uniform distribution in the range [0,1] (initial density $\rho_0 = 0.5$). The system is first run for 10^6 time-steps for activity to settle and reach the thermodynamic limit. Then the system is run for another 10^6 time-steps to calculate the average of states over time and space. The same procedure is repeated 28 times for each value of λ starting with different initial conditions and the λ-dependent ρ is found by taking the average of these runs.

The λ-dependent ρ is shown in Fig. 3.2(a). Conway's GoL is well known for its long transients and its subcritical nature eventually leads it to a phase dominated by quiescent states and sparsely distributed stable or periodic structures called still life and oscillators, respectively. We call this phase inactive asymptotic state. In the range $0.875 < \lambda \leq 1$, Logistic GoL eventually reaches to such inactive phase. ρ remains almost constant in this range, as shown in Fig. 3.2(a).

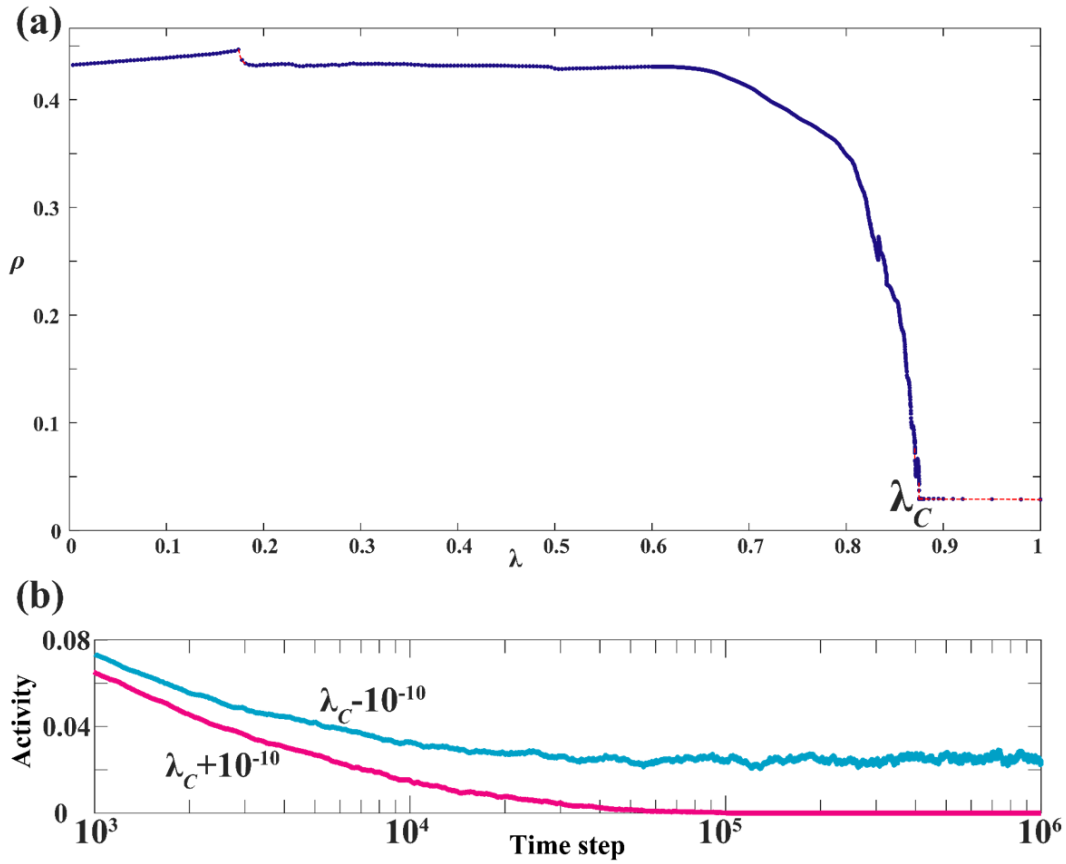

Figure 3.2: (a) The asymptotic density, ρ, in the Logistic GoL with respect to the tuning parameter λ. The blue dots correspond to numerical result while the red dashed lines are guide for the eye. (b) Semi-logarithmic plot of average activity versus the time step.

At $\lambda = \lambda_C = 0.875$ there is a critical transition in system's behavior accompanied with a change in the average density. From this point on the density starts increasing and the dynamics of the system keep showing qualitative and quantitative changes with respect to Conway's GoL, as seen also by snampshots in Fig. 3.3. As λ is decreased down to ~ 0.8 the dominance of quiescent phase fades while the activity percolates. This leads to emergence of chaotic regions consisting of rapidly changing disordered states, which we name as flickering phase. After this point, the activity starts decreasing while the average density plateaus to a much higher value, $\rho \approx 0.44$. This value can in turn be justified by using the adapted single site mean field approximation, already discussed in Sec. 3.1.

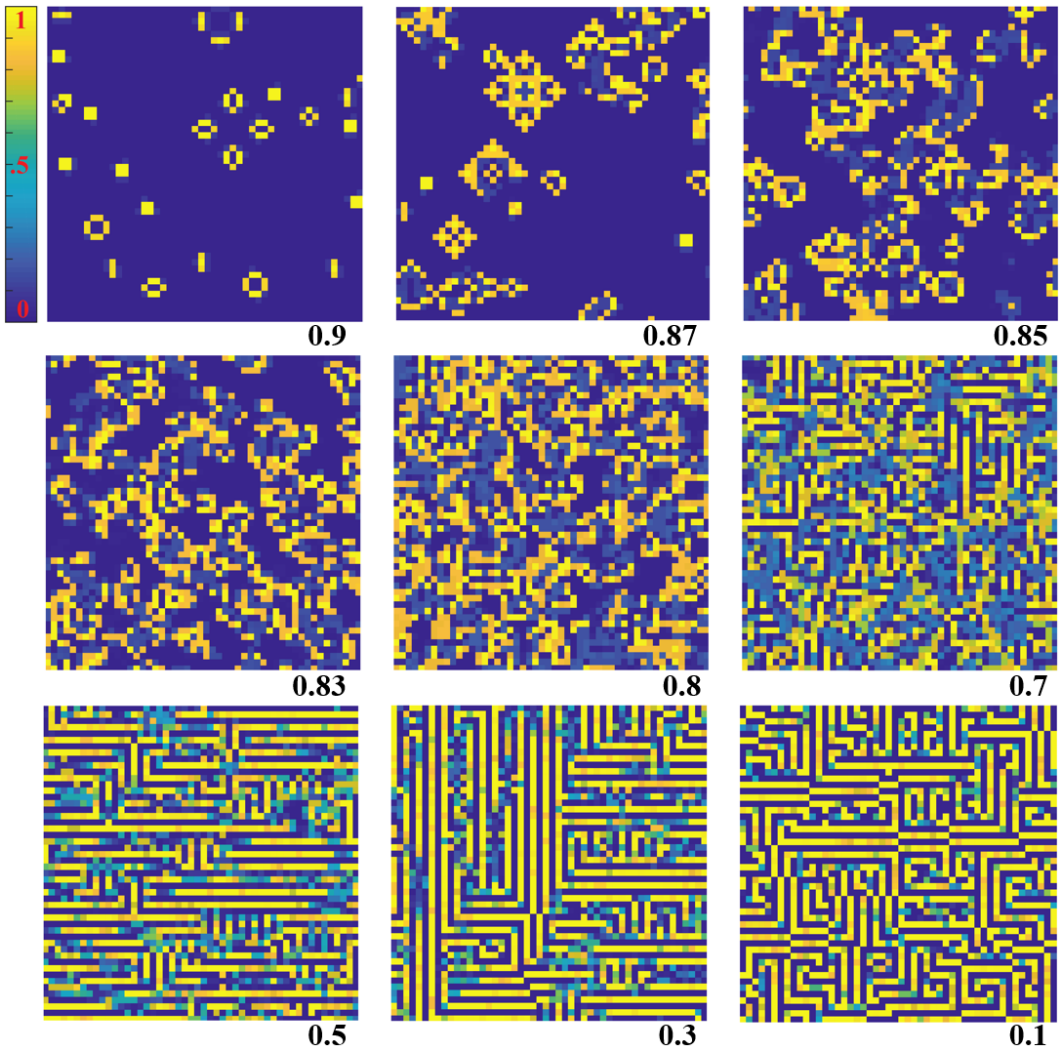

Figure 3.3: Random snapshots of asymptotic states of Logistic GoL at different λ values.

Tuning λ down further gives rise to domain-like structures of stable horizontal and vertical stripe patterns that interact with networks of flickering states at their boundaries (see Fig. 3.3). Similar stripe patterns were observed in the asynchronously updated version of GoL [29].The flickering states can also propagate over the stripe patterns while changing them, allowing the system to comprise both ordered (stripes) and chaotic (flickers) phase in it simultaneously.

It is important to notice that stripe patterns are actually a new dynamically

stable configuration of the system. Dense sites self organize in orthogonal orientations and each of them neighbors only two other dense sites by remaining in the stability regime ($t_1 < m < t_2$), whereas the surrounding empty sites that actually make up the remaining of space, keep decaying as their neighborhood mostly consists of six dense sites. This way the sites get correlated and help maintain larger scale stable domains of such patterns. We perform a more quantitative analysis of pattern formation on Sec. 3.3.

The Cantor set that defines the state-space becomes simply connected at $\lambda = 0.5$ which is accompanied with a sudden change in the average density. As λ approaches ~ 0.18 the flickers become isolated and the system makes transition to an asymptotic state that has very low activity. In fact, the density of this asymptotic state depends on initial conditions. Starting with uniform distribution results in linear dependence of ρ on λ.

To further clarify the transition at $\lambda_C = 0.875$, we calculate the time dependent average activity of the system for $\lambda = \lambda_C + 10^{-10}$ and $\lambda = \lambda_C - 10^{-10}$. Here the activity at time step t is calculated by first taking the difference of states at each cell by their corresponding values 60 time steps before and then finding the average of the absolute values of these differences. This way one gets zero average activity when the system reaches the inactive asymptotic state with oscillators having periods that are divisors of 60. All of the 28 runs reach inactive asymptotic state at approximately 10^5 steps when $\lambda = \lambda_C + 10^{-10}$ while all of the 28 runs remain active after 10^6 steps when $\lambda = \lambda_C - 10^{-10}$. Semi-logarithmic plots of average activities are presented in Fig. 3.2(b). This clearly shows that λ_C marks the point of sudden departure from subcritical nature of Conway's GoL to an active asymptotic behavior.

In Fig. 3.4(a) we present close inspection around λ_C which reveals that there are many other transitions that are present in $\lambda < \lambda_C$. To understand the source of the transition at $\lambda_C = 0.875$ and the subsequent transitions we must focus on conditions that change the operation regimes of the system. As the tuning parameter alters the rate of change in states, the neighborhood sums m made up by these states are also tuned.

Changes in operation regions occur when m sums cross any of the limits t_1, t_2 or t_3. For example, if m is slightly less than t_3 then the corresponding state will grow but if, upon tuning λ the same sum becomes a value slightly larger than t_3, the site will decay. Hence, $m = t_3$ will correspond to transition between two significantly different pathways in the system. The more these "equalities" occur the greater will be the impact on the global dynamics.

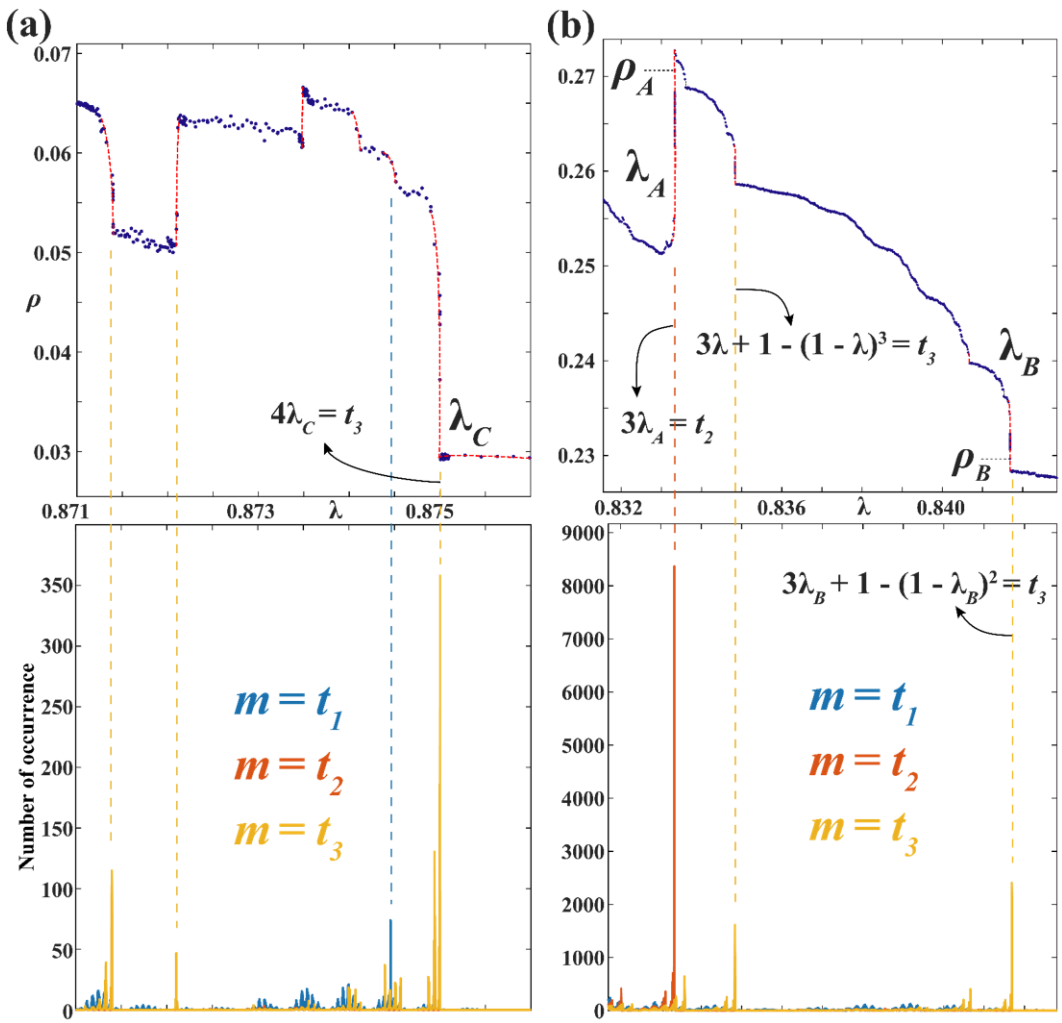

Figure 3.4: Top panel: two magnified regions of the plot in Figure 3.2(a). Bottom panel: the number of times the neighborhood sum m is equal to either t_1, t_2 or t_3 with respect to λ. (a) refers to the inactive-active transition point and (b) is a magnified region where active-active transitions occur. Equations refer to polynomial forms of m sums that change their operation regions.

To numerically investigate the values of λ where significant changes are expected, we start from a 1000×1000 uniform initial state and run the system for a 1000 steps. Then we run the system for another 1000 steps while recording the number of occurrences where m is equal to t_1, t_2 or t_3 up to a precision 10^{-6} that is also the increment with which λ is tuned. The number of occurrences versus λ is plotted at the bottom panels of Fig. 3.4. As we expected, there is indeed a sharp peak at $\lambda = \lambda_C$ in the number of occurrences of $m = t_3$. Also the other transitions are accompanied with their relevant peaks.

Yet we can offer an alternative approach to explaining why $m = t_3$ has a peak at $\lambda = \lambda_C$. We start by restating that at these values of λ the system is dominated by quiescent phase (regions of zeros) with sparse activity. States having values λ keep forming as a result of single growth operation on zeros at the boundaries where active sites meet quiescent phase. Indeed states involving less number of operations are formed more frequently than those needing more operations. In other words, states having lower polynomial degree on λ are more frequent than others. Hence the transition at $\lambda_C = 0.875$ can be explained by $4\lambda_C = t_3$, which corresponds to a quite frequent neighborhood populated by four λ states and four zeros. As λ is tuned down the operation of this sum changes from decay to growth, and any cell with such neighborhood starts growing instead of decaying, thereby altering the dynamics.

Another substantial change occurs at $\lambda_A = 5/6$ when $m = 3\lambda_A = t_2$ (a neighborhood of three λ states and five zeros), as seen in Fig. 3.4(b). Here one of the frequently occurring sums changes its region from growth to stability and leads to sudden decrease in density as λ is decreased. This transition is different from the one at λ_C as the system has active asymptotic states both before and after. Another related transition is present at $\lambda_B \sim 0.842$ which can be understood by employing the second order values of the Cantor set, namely $\{(1-\lambda)^2, \lambda(1-\lambda), \lambda + (1-\lambda)^2, 1-(1-\lambda)^2\}$. Then the corresponding equation is $3\lambda_B + 1 - (1-\lambda_B)^2 = t_3$. This transition in turn can be related to yet another transition at $\lambda \sim 0.834$ in which the third order values are employed in the equation $3\lambda + 1 - (1-\lambda)^3 = t_3$. The magnitude of change in the density

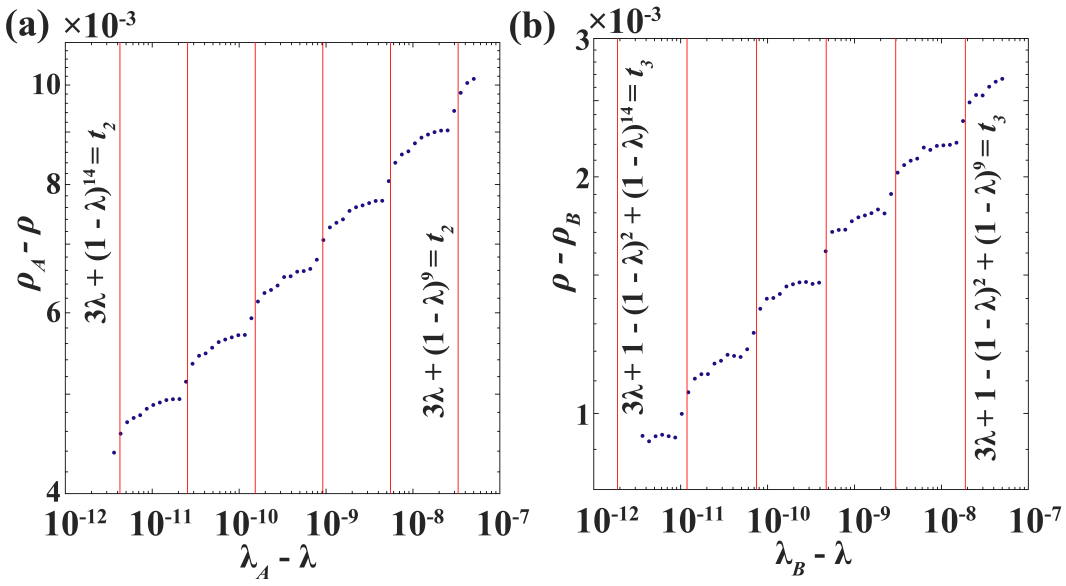

Figure 3.5: Log-log plot of the transition at λ_A and λ_B present in Figure refsum-transitions. The red vertical lines delineate micro-transitions (see the text).

decreases as the sums m involve more and/or higher order terms and hence occur less frequently. Taking this idea further, one can claim that every transition point is accompanied by infinitely many nearby transition points involving ever less frequently occurring higher order terms of the Cantor set. This claim is supported by the log-log plots of changes in the density versus changes in λ near the critical points λ_A and λ_B presented in Fig. 3.5. Here, adding the smallest nonzero element of the n^{th} order Cantor set, $(1-\lambda)^n$, to the original equations result in new equations corresponding to accompanying micro-transitions shown by red vertical lines. Each deterministic transition follows a linear trend in the logarithmic scale which is similar with the power-law behavior of critical transitions in stochastic systems while the presence of cascade like micro-transitions yields a qualitatively different self-similar nature.

3.3 Pattern Formation

In this section, we define a neighborhood correlation function and analyze the λ-dependent dynamics of self organized pattern formation in the Logistic GoL:

$$C\left(i,j\right)=\sum_{i'}\sum_{j'}\left|s\left(i^{'},j^{'}\right)-s\left(i,j\right)\right| \tag{3.5}$$

where $s(i,j)$ denotes the state at the corresponding coordinates and $i^{'}$ and $j^{'}$ indices run through the Moore neighborhood for every site.

Low correlation values $C(i,j)\in[0,2]$ refer to almost or fully homogeneous regions, with the stable ones being quiescent states. High correlation values $C(i,j)\in[6.5,8]$ are unstable configurations in the Logistic GoL belonging to either overcrowded or exposed states. The sites belonging to stripe regions are states close to the limiting values of the state space, with six "opposite" neighbors, therefore the values $C(i,j)\in[4.5,6.5]$ account for this pattern. The remaining values of correlation mostly refer to the disordered chaotic groups of highly active states, which we call flickers. We perform simulations of a 256×256 lattice with periodic boundary conditions, running 10^4 steps to thermalize and another 10^4 steps (if inactive asymptotic state is not yet reached) to average the correlation for each cell, and run 10 trials for every λ. Fig. 3.6 shows a histogram of the correlations' distribution in the lattice indicating the emergence of different phases as λ is tuned, where initially sparse domains mix with highly active disordered states that percolate in the system and eventually generate packed stripes in accordance with equilibrium conditions of the Logistic GoL. These self-organized patterns consist of empty states due to overcrowding and crowded states that maintain their stability with their neighborhood sums stabilizing between t_1 and t_2. Pattern formation at the same time indicates the bistability of the system despite an expanded state space. The system ends up stabilizing in an ordered fashion through spatial correlations and occupies a very limited range of $\tilde{\mathbf{S}}$, namely the values close to 0 and 1 (see also Fig. 2.4).

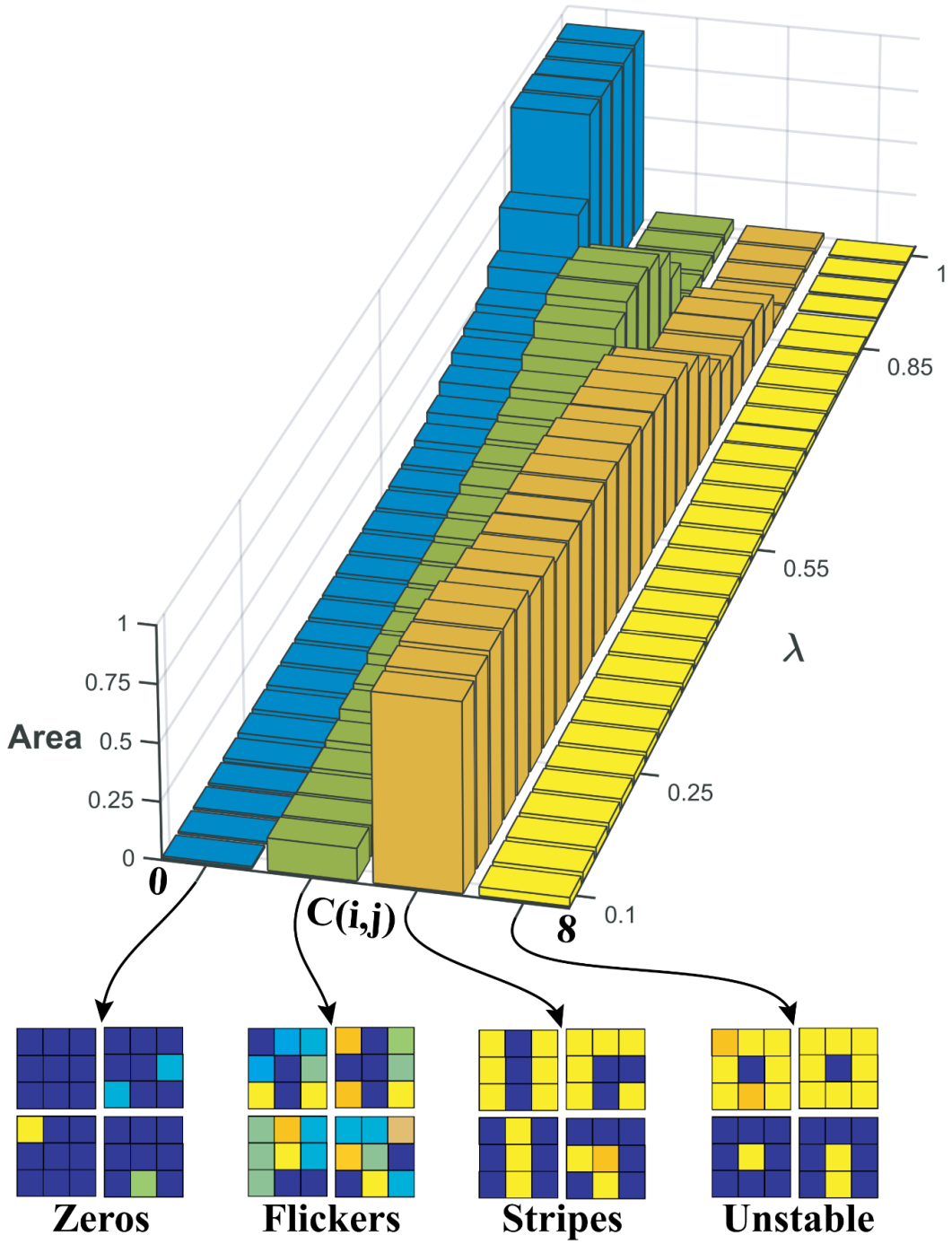

Figure 3.6: Histogram showing the distribution of different phases in lattice versus λ, measured using Eq. 3.5. Blue bins represent almost/fully homogeneous phase, whereas green and orange bins represent the disordered flickering states and stripe regions, respectively. Yellow bins refer to unstable configurations in GoL.

Chapter 4

Self-Organization

In this chapter we develop a method that makes crucial use of the operator notation for analyzing self organizing morphologies that emanate as the parameter is tuned. Initially we apply this method to the Glider, which already exists in Conway's GoL, and then to a new propagator which appears in a different range of λ.

4.1 Autocatalytic Interactions: The Glider

To understand how self-organized structures arise in the Logistic GoL, we formulate the tuning parameter range where propagators adaptively survive by investigating their local interactions. Propagators are actually the utmost indicators of self-organization in CA [40, 34]. We first consider the Glider, an emergent propagator transmitting activity in the long range and also the key component in computational properties of Conway's GoL. [22, 41] Glider is translated one diagonal cell every four steps.

In our model, it preserves its direction, speed and periodicity in a continuous range of λ. As seen in Fig. 4.1 for $\lambda = 0.8$ Glider has a similar structure, yet with different numerical values due to the altered updating rate. Note that behind

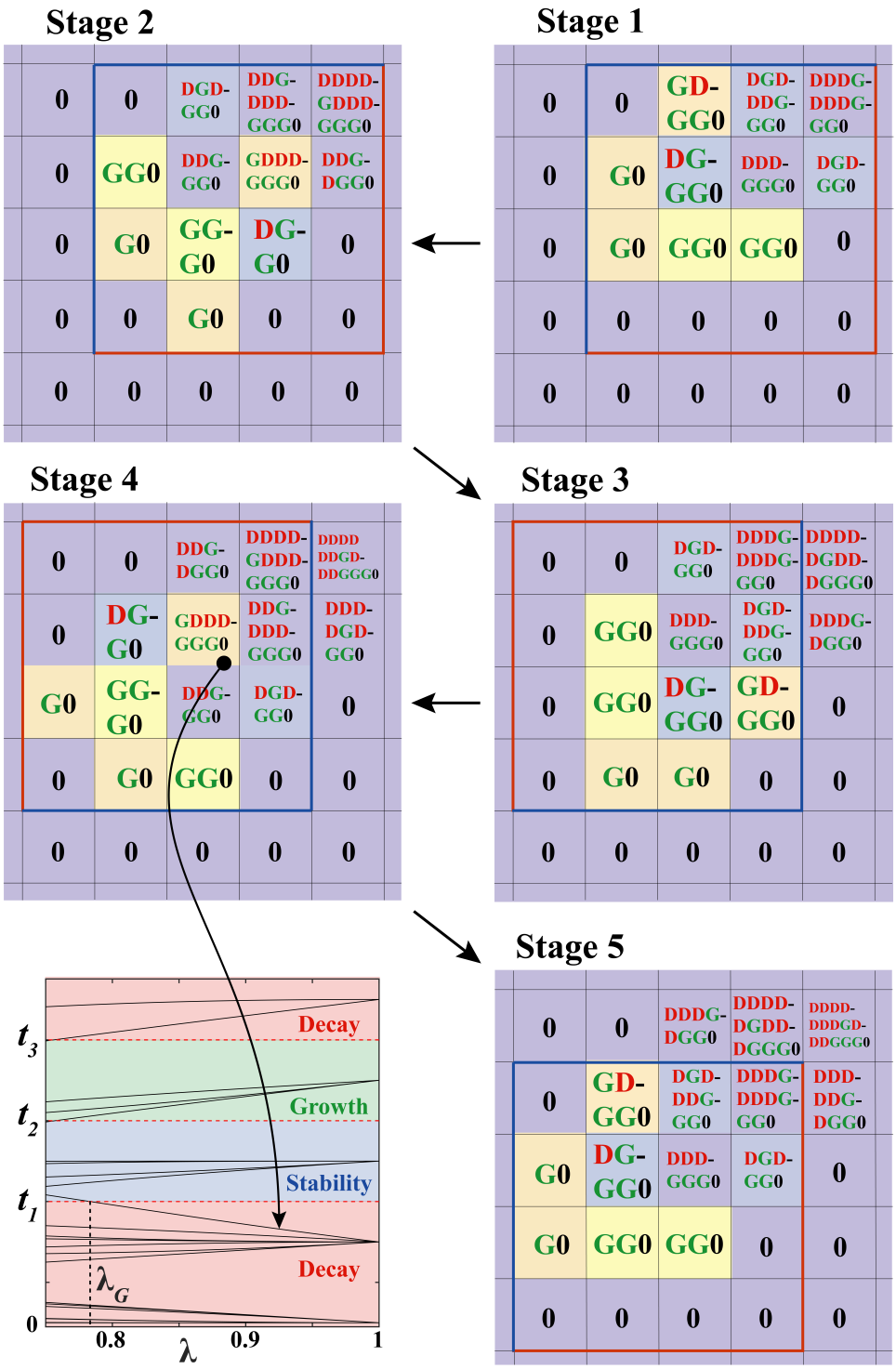

Figure 4.1: Five stages of evolution of the Glider in the Logistic GoL for $\lambda = 0.8$. The set of operations is preserved for the initial and final stages. Bottom graph: Neigborhood sums versus λ. The first change in operation regions of sums occur at $\lambda = \lambda_G$, corresponds to the cell shown by the arrow.

any stable, oscillating or propagating structure, there is a pertaining finite set of local interactions involved. We quantify these interactions by investigating the corresponding neighborhood sums m under the operations employed by the rules. Considering the polynomial representation of states (operator notation introduced in Sec. 2.2) is essential for this study because it allows us to extract quantitative information about the local interactions of complex structures.

To find the parameter range in which the Glider can be preserved, we record the operations on each cell for every time step as this structure propagates in a field of quiescent states. This analysis is presented in Fig. 4.1 with stability operations ommited. Each decay or growth operation increases the polynomial order of the state by one degree. The m for each site can thus be expressed in terms of λ dependent polynomials. Once Glider "leaves" a certain region, the visited sites will keep decaying indefinitely due to exposure (underpopulation) and the neigborhood sums of these cells trivially fall in the decay region ($m \approx 0$). Active cells, which lead the propagation mechanism, make up a finite set of recurring nontrivial operations corresponding to this structure, equivalent to attractors in dynamical systems [37, 42]. Due to their self-generating character, we name these operations as autocatalytic interaction sets. As λ is tuned, if these outer-totalistic sums remain within their corresponding regions of operation, it means that the supposed operations will keep recurring, hence the Glider can still propagate under such growth/decay rate. Its structure will be altered when the first sum changes its operation region.

As seen in Fig. 4.1 (see the graph), the first sum which changes the dynamics and breaks this emergent behavior occurs at $\lambda_G \sim 0.783$ where a polynomial of eleventh order in λ crosses t_1 from decay to stability. The order of this polynomial is dictated by **DDDDGDDDGGG0**, which is the highest order state in the Moore's neighborhood of the cell changing its operation regime. Notice that, the presence of symmetries in this framework reduces the number of unique interactions significantly. These symmetries are actually present between odd and even states of the structure, being transposed versions of each other, and are highlighted by the red and blue contours in Fig. 4.1.

4.2 Rayfish: An Emerging Propagator

By tuning the parameter, we further notice the step-by-step emanent self-organization of a propagator that is only partially present in Conway's GoL. This period-36 orthogonal propagator, named "Rayfish" after its shape and dynamics (see Fig. 4.2(a)), appears in a short, yet continuous range $\lambda_A < \lambda < \lambda_R$. Here, $\lambda_A < \lambda$ supports the main propagation mechanism of the Rayfish, where a column of three λ states gives birth to another λ next to them. On the other limit, $\lambda_R \sim 0.841$ is the solution to another eleventh order polynomial equation in λ, computed using the analysis method presented in the previous session. 22 of the 36 links in the Rayfish loop are also present in Conway's GoL, including the 6 consecutive steps (from 11 to 17) that connect the largest stages. These stages are easily noticed in active regions of Conway's GoL. On the other hand, stages from 24 to 29 are very simple structures that are easily reached, making Rayfish a very frequent attractor which contributes to the large increase in density at λ_A as λ is increased.

In Fig. 4.2(b), using the recorded neighborhood sums of Rayfish (similarly as with the Glider), the supported stages are shown as λ is varied. The structure is set only once to propagate in a field of empty states and, by recording the operations, we can extrapolate information about every stage of Rayfish in the whole parameter range. Having obtained the results, from a reverse perspective one can see how tuning λ down gets the neighborhood sums coupled step by step until they reach the autocatalytic regime, where all the stages are supported and there is no interaction that breaks the loop. Outside the range $\lambda_A < \lambda < \lambda_R$ stages start breaking down, making this attractor not reachable anymore, while the number of neighborhood sums changing operation regions increases and further deteriorates the loop. Thus, it is important to emphasize not only the robustness and inevitability of this propagator inside its operating range, but also the vulnerability and its incomplete unveiling outside that range. Being quite abundant while possessing sheer complexity are two properties of this emergent system which, instead of remaining mutually exclusive, counter intuitively start supporting each other.

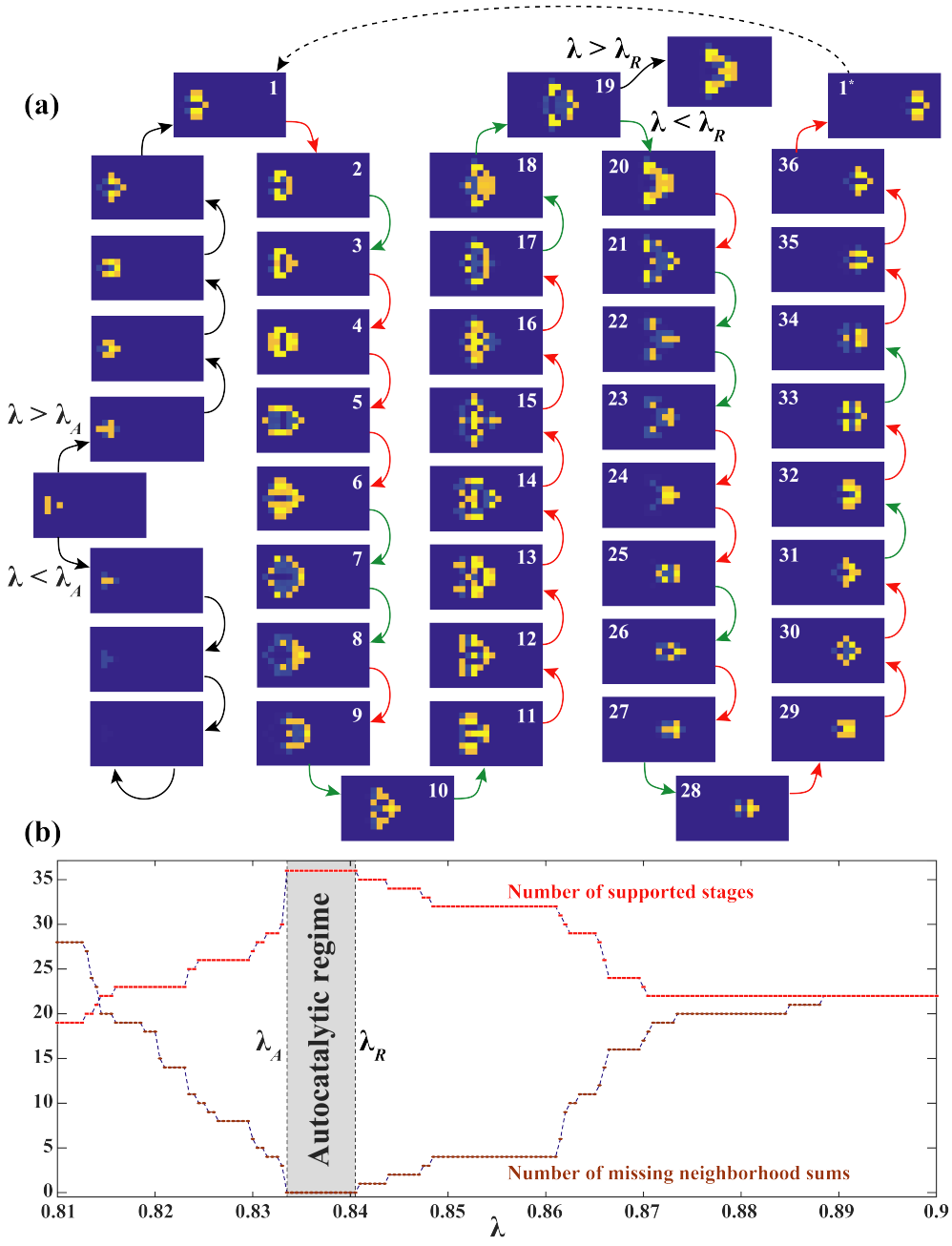

Figure 4.2: (a) Formation of period-36 propagator named Rayfish from simple initial conditions. The red arrows indicate the steps present also in Conway's GoL. 1* and 1 denote the same but translated states. (b) Red lines represent the number of Rayfish stages that are dynamically reachable versus λ. The stages supported by the neighborhood sums form an autocatalytic loop only in the shaded interval. Outside this interval the neighborhood sums change their operation regions, as shown by the brown lines.

The development process itself and properties of Rayfish make it a suitable abstract model for investigating the origins of life scenarios based on self-organizing autocatalytic reaction sets [43]. In the context of CA, Rayfish is an epitomic example of how local sites get coupled in a consequent series of interactions that generate a self-sustained loop. There is a spatio-temporal synchronization of values and operations, which effectively exploits the different symmetries of the framework, thereby introducing consonance in a higher hierarchy even though only local interactions are involved [44].

4.3 Further Emergent Behavior

Exploring the rules of Logistic GoL for $\lambda > 1$ generates numerical values beyond the interval [0,1], however with many other autocatalytic interaction sets which emerge in particular regimes and exploit the symmetries of the cellular space in different configurations. Fig. 4.3 shows three different morphologies related to propagation and self-replication phenomena.

The structures shown in Fig. 4.3 are not the only ones present in this regime, however they appear very frequently when the system is set to run from random initial conditions. The first one at λ=1.3 is a structure with a replication symmetry occurring also in the well known the Parity Rule with von Neumann neighborhood [34]. It is quite remarkable to observe this similar topology in a framework which is governed by quite different rules and a different neighborhood geometry. The orthogonal propagators are the only structures that persist in the asymptotic states when $\lambda = 1.5$. They are very similar to one another and propagate at the photonic speed in CA. This is another important parameter regime that demonstrates how coupled interaction sets are able to emerge from a "primordial soup" and be the only ones to survive in the asymptotic state. The last case is a type of structure which not only propagates, but also generates adjacent copies of its units in a certain configuration. This type of structure is the only prevailing architecture of asymptotic states at $\lambda = 1.6$.

These examples serve as strong indicators that the influence of a parameter can be more effective than just related to a specific type of transition. In such systems, tuning the pace of decay and growth yields different types of interactions that in turn get coupled to generate a considerable variety of artificial life structures.

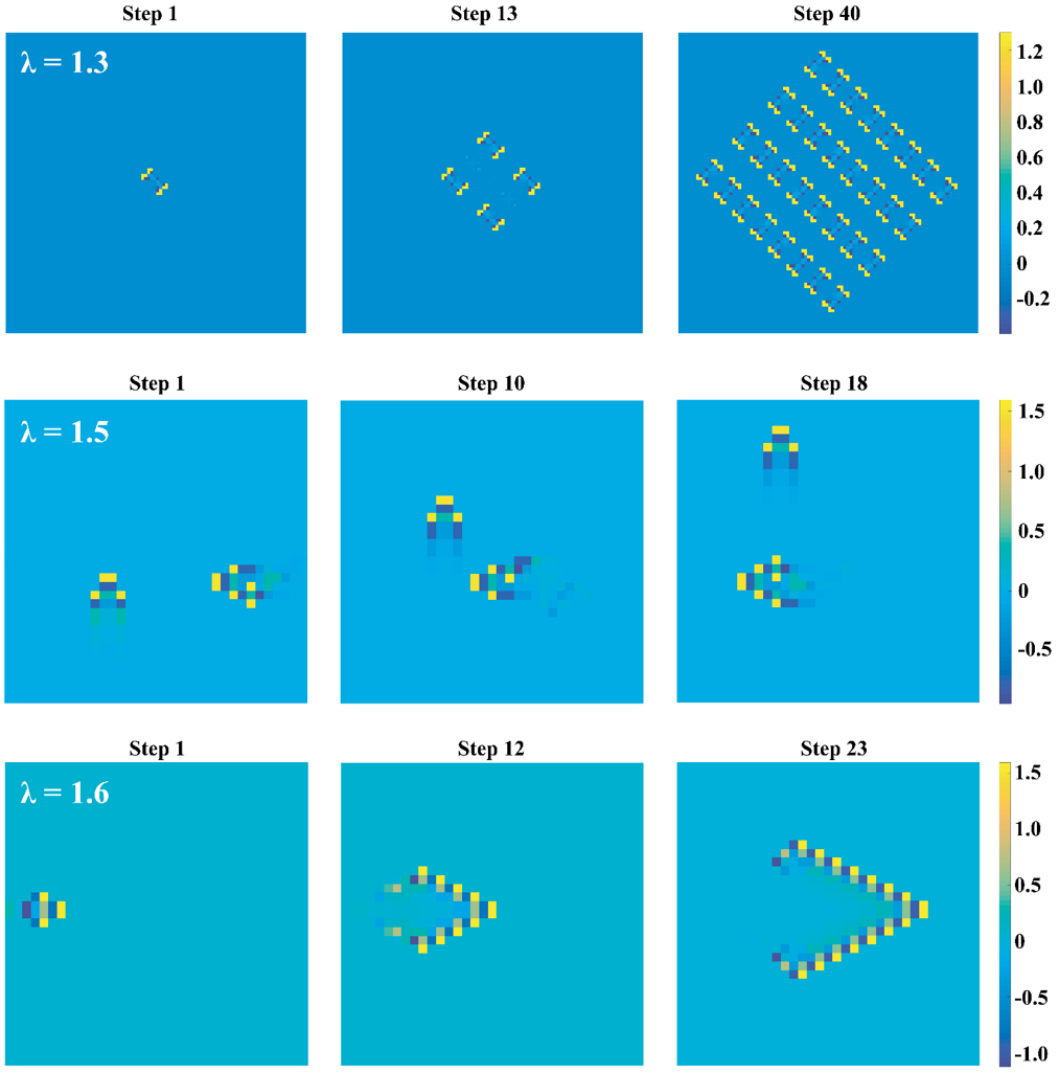

Figure 4.3: Snapshots showing simple self-replicating structure (top) at $\lambda = 1.3$, propagating ships at $\lambda = 1.5$ (middle) and another structure which instantaneously self-replicates and propagates at λ=1.6 through the lattice (bottom).

Chapter 5

The Logistic Rule 90

This Chapter introduces a detailed analysis of the logistic version of Rule 90, presented in Sec. 2.3. We discuss the transitions induced by the tuning parameter and how self-organization in this system is particularly related to transitions between Wolfram's universality classes.

5.1 The Model

It is very straight forward to implement our framework int Rule 90, an outer totalistic 1D elementary CA in which the state of a cell is determined by the sum of its two nearest neighbors [45]. The actions correspond to decay and growth if the modulo 2 of the sums are 0 and 1, respectively. Introducing λ transforms the neighborhood space $\tilde{\mathbf{M}}$ into a continuous set in the range [0, 2] populated by two-fold convolution of the λ-dependent Cantor set. We assign the growth interval to the range [0.5, 1.5] sandwiched between two decay regions, as shown in Fig 5.1. Here the limits of the operation regions are denoted as t_1 and t_2 respectively. Note that the rule space here is $\tilde{\mathbf{R}} = \{\mathbf{D}, \mathbf{G}\}$, consisting of two operations only.

This system is simpler than Logistic GoL, hence the respective simulations are presented in a time-space diagram with the parameter tuned as time evolution

(a)

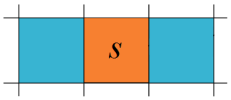

s: state of the chosen site

(b)

	Wolfram's Rule 90		Logistic Rule 90	
	Condition	Δs	Condition	Δs
Decay	$m = 0, 2$	$-s$	$m < t_1 \vee m > t_2$	$-\lambda s$
Growth	$m = 1$	$1-s$	$t_1 \leq m \leq t_2$	$\lambda(1-s)$
Operation Regions				

Figure 5.1: (a) Two nearest neighboring sites making up the minimal neighborhood ($\phi = 1, D = 1$) in Rule 90. (b) Table shows the conditions and equations for the operation regimes: decay and growth. The difference equations are rescaled by the parameter λ and the operation regimes are bounded by parameters denoted as t_1 and t_2.

occurs. We show how dynamics of the Logistic Rule 90 changes when λ is decreased as the system starts from a single populated cell. Even though λ is tuned while the system is run, initially the system evolves in the same fashion with the original Rule 90 producing the fractal object called Sierpinski triangle.

5.2 Phase Transitions

5.2.1 Emergence

At $\lambda = 0.75$ dynamics of the system changes substantially for the first time. To understand this change, we plot all unique sums produced by adding two elements from the second order Cantor set assuming that these are the most frequently occurring ones. Any of the sums changing operation region as λ is varied could induce different dynamics in the system. As seen in Fig. 5.2(b), at $\lambda = 0.75$ two of the sums cross t_1 and t_2 lines, both going from decay to growth. The crossing sums correspond to formulas $2(1 - \lambda) = t_1$ and $2\lambda = t_2$. In fact, all crossings come in symmetric pairs because of the symmetry in both the Cantor set and the rules of this particular system. The next crossing occurs when the sum of the elements $(1 - \lambda)$ and $(1 - \lambda) - (1 - \lambda)^2$ is equal to t_1 which corresponds to

$\lambda = 1/\sqrt{2}$. This point is also accompanied with a substantial change in dynamics. The arrows extended from the transition points (see Fig. 5.2(a-b)) also coincide with different regimes of textures emerging in the system. The next significant change in dynamics, however, occurs for a different reason. To understand this, we need to consider the possibility of having oscillating states.

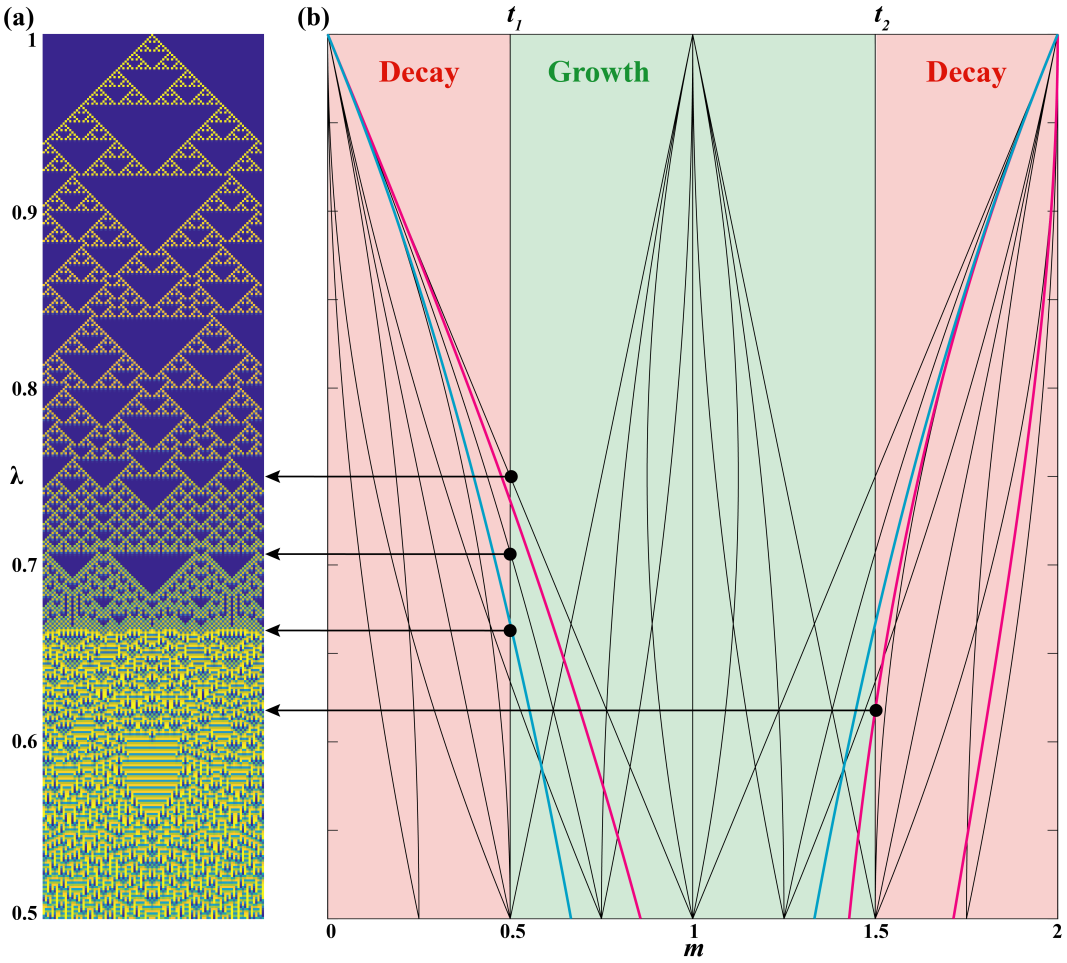

Figure 5.2: (a) Time evolution of Logistic Rule 90 accompanied with decrease in λ. (b) Thin black lines represent all unique sums that can be constructed by adding to elements from the second order Cantor set. The cyan lines represent the $2s_1$ and $2s_2$ sums of period-2 stripes (see the text). The magenta lines represent the $2s_1$, $2s_2$ and $2s_3$ sums of period-3 stripes. Arrows attribute the important changes in dynamics to crossings of sums between decay and growth operations.

The simplest case would be having states with value s_1, dominating a region of space, altogether changing their values to s_2 and then returning back to s_1 and repeating this oscillatory behavior. Assuming that $s_2 > s_1$, this kind of period-2 stripes (in time domain) are supported if $\mathbf{G}s_1 = s_2$ and $\mathbf{D}s_2 = s_1$. Solving these equations simultaneously one gets $s_1 = (1-\lambda)/(2-\lambda)$ and $s_2 = 1/(1-\lambda)$. However, to be in the correct operation regime, we also need to have $2s_1 > t_1$ and $2s_2 > t_2$. The sums $2s_1$ and $2s_2$ are plotted with cyan lines in Fig. 5.2(b). One can see that $2s_1 > t_1$ holds for $\lambda < 2/3$ while $2s_2 > t_2$ holds for $\lambda > 2/3$. This makes $\lambda = 2/3$ a very special point where period-2 stripes are supported. Indeed, running the system with $\lambda = 2/3$ (not shown here) results in complicated dynamics dominated by period-2 stripes. Same arguments apply for checkerboard pattern but this time with $2s_1 < t_1$ and $2s_2 < t_2$. One can spot both checkerboard pattern and period-2 stripes in the vicinity of $\lambda = 2/3$ but they quickly fade because they lack autocatalytic sets as described above. The cyan lines in Fig. 5.2(b) representing the sums that support these patterns resort in decay for $\lambda < 2/3$ and growth for $\lambda > 2/3$. Hence, the average density increases as one passes over $2/3$ while decreasing λ.

Decreasing λ further we hit a point where period-3 stripes [46] emerge and start dominating the system. One way of getting a period-3 stripe is to have $\mathbf{G}s_1 = s_2$, $\mathbf{G}s_2 = s_3$ and $\mathbf{D}s_3 = s_1$. Solving these equations simultaneously one gets $s_1 = (1-\lambda)(2-\lambda)/(\lambda^2-3\lambda+3)$, $s_2 = ((2-\lambda)/(\lambda^2-3\lambda+3)-\lambda)/(1-\lambda)$ and $s_3 = (2-\lambda)/(\lambda^2-3\lambda+3)$. Being in the correct operation regime requires conditions $2s_1 > t_1$, $2s_2 < t_2$ and $2s_3 > t_2$. The sums $2s_1$, $2s_2$ and $2s_3$ are plotted with magenta lines in Fig. 5.2(b). All conditions are satisfied starting with the point where $2s_2 = t_2$ that corresponds to equation $\lambda^3 - 2\lambda + 1 = 0$ which has a root at $\lambda = (\sqrt{5}-1)/2$ (the golden ratio). As seen in Fig. 5.2(b), from this point on, period-3 stripes indeed appear and start dominating the system as λ is tuned down.

Note that, the values s_1, s_2 and s_3 are not members of any low order Cantor set. In fact, their autocatalytic nature forces the system to approach these values using higher orders of the Cantor set. In other words, very high order elements of the Cantor set that are normally extremely rare, get boosted to the point where

they start to prevail the system dynamics. This is another excellent example of emergent behavior.

5.2.2 Class Transitions

At $\lambda \sim 0.6$ the period-3 stripes reach their peak size while localizing chaotic regions up to a point where the latter become propagators interacting with each other in a complex fashion. These propagators become more apparent after a transformation introduced in Fig. 5.3. Here we make use of the fact that $s_1 + s_2 + s_3 = 2$. Then instead of plotting s^t that corresponds to state at time step t, we plot $|s^{t-1} + s^t + s^{t+1} - 2|$ in which case stripes appear as homogeneous fields of zeros. To reveal the rich dynamics around $\lambda \sim 0.6$ we start with 2500 cells having uniform distribution between [0,1]. Then in 10000 steps we *increase* λ from 0.575 to 0.625.

In Fig. 5.3 we present four small snapshots of this system. One can see that around $\lambda \sim 0.587$, period-3 stripes (blue regions) have no dominance. This is because the gap between the values s_1, s_2, s_3 and the Cantor set elements that are closest to them are too wide to be bridged with autocatalysis. As λ is increased, period-3 stripes smoothly grow in size while propagators start appearing. Hence, in the context of canonical classification of CA [16] , we observe a transition from "chaotic" Class III phase to complex "life-like" Class IV phase. This kind of transition was investigated earlier in the context of "computation at the edge of chaos" where Langton introduced a CA parametrization technique [47]. The novelty of our application is that we achieve the same transition while keeping the same rules and tuning a single parameter continuously.

The range $0.595 < \lambda < 0.605$ is dominated with a period-18 propagator that moves in the field of period-3 stripes, as shown in Fig. 5.3(a-b). The autocatalytic interactions of this propagator are more complicated compared to those of Rayfish which propagates in the field of zeros. $\lambda \sim 0.605$ marks an unprecedented case where the autocatalytic interaction set of period-18 propagator is broken while a different set supporting a new period-48 propagator is formed

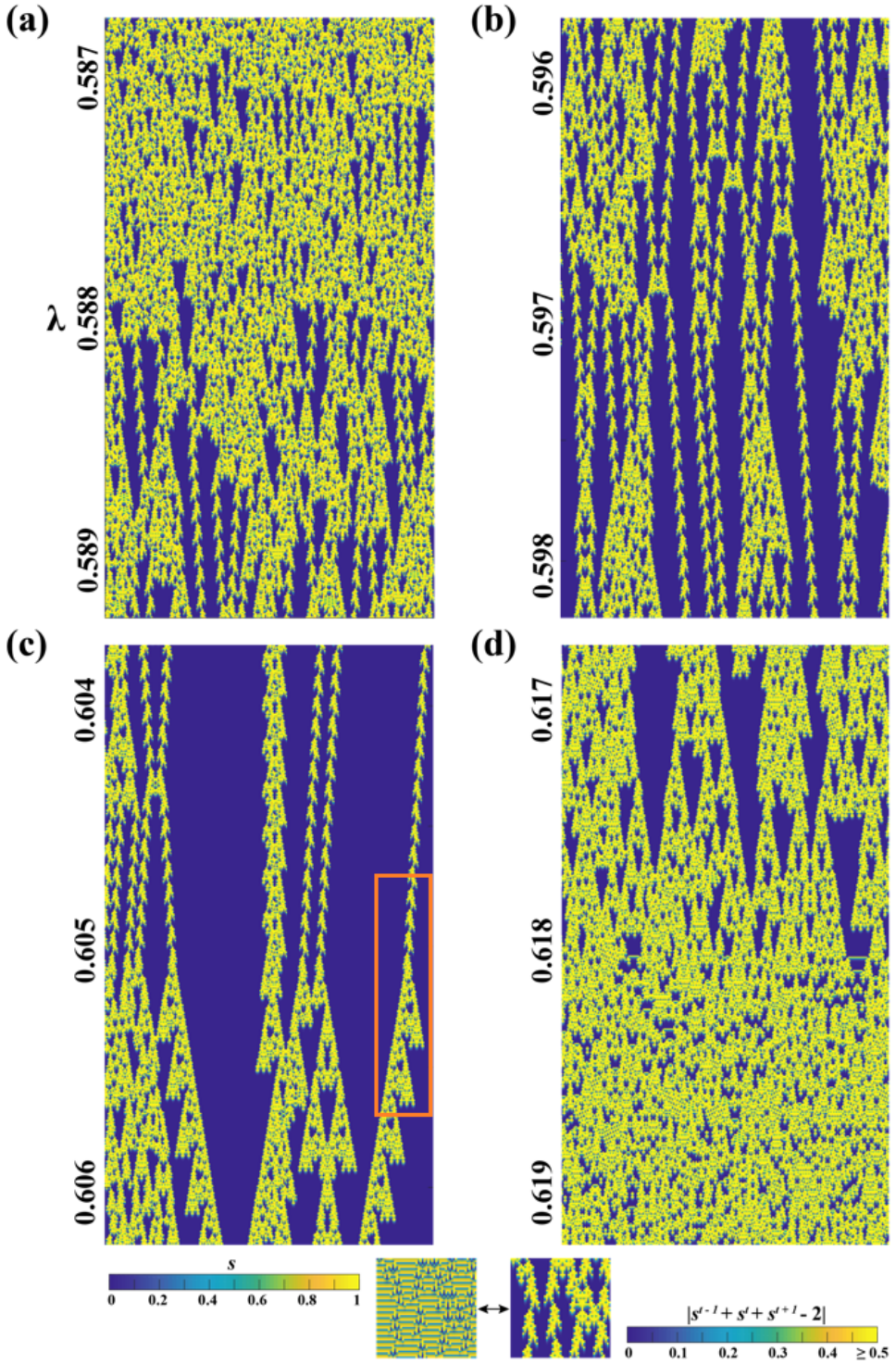

Figure 5.3: Four snapshots of larger implementation of the same system whereby in 10^4 time steps λ is increased from 0.575 to 0.625, starting with 2500 cells having random initial values of $\rho_0 = 0.5$, and periodic boundary conditions. Bottom Panel: Transformation that maps period-3 stripes into a uniform field for better visualization.

(see Fig. 5.3(c)). This resonates with the idea of punctuated equilibrium where an organism acquires substantial change in a short period of time to adapt to a new fitness landscape [48, 49]. The period-48 propagator dominates the system dynamics until we reach $\lambda = (\sqrt{5} - 1)/2$ where they disappear since the system stops supporting period-3 stripes that act as their habitat.

Chapter 6

Discussions and Outlook

Next to the Logistic GoL, just by changing the stability and/or growth regimes one can generate many of the possible birth/survival rules of other life-like CA, and exploit the approaches followed in this work to explore novel behavior in this discrete realm. A further examination would lead to a plethora of patterns, propagators and other self-organizing structures that appear under different rules and can provide helpful insights on suggesting phenomenological models of complex behavior. In this section we briefly discuss a group of several CA models in which λ can be implemented in a straightforward fashion. The discussions are very qualitative aim to reflect the expanding complexity that our application offers.

6.1 34 Life

Rule 34 Life is a famous Class III automaton in the family of Life-Like CA. It is often written as B34/S34 [23], thus indicating the conditions of birth and survival. In this model, the state of a site evolves according to the set of equations below:

$$s(\mathbf{r}, t+1) = \begin{cases} 1\ ;\ m(\mathbf{r}, t) = 3, 4. \\ 0\ ;\ m(\mathbf{r}, t) = 0, 1, 2, 5, 6, 7, 8. \end{cases} \tag{6.1}$$

This model is known to eventually generate chaotic behavior. However, there are also stable, oscillating and propagating structures that appear in sparse regions of the system. We perform the rule transformation in a similar way done with Conway's GoL, obtaining the following form:

$$\Delta s = \begin{cases} \lambda(1-s);\ 2.5 < m \leq 4.5. \\ -\lambda s \quad\quad ;\ 2.5 \leq m, or\ m > 4.5. \end{cases} \tag{6.2}$$

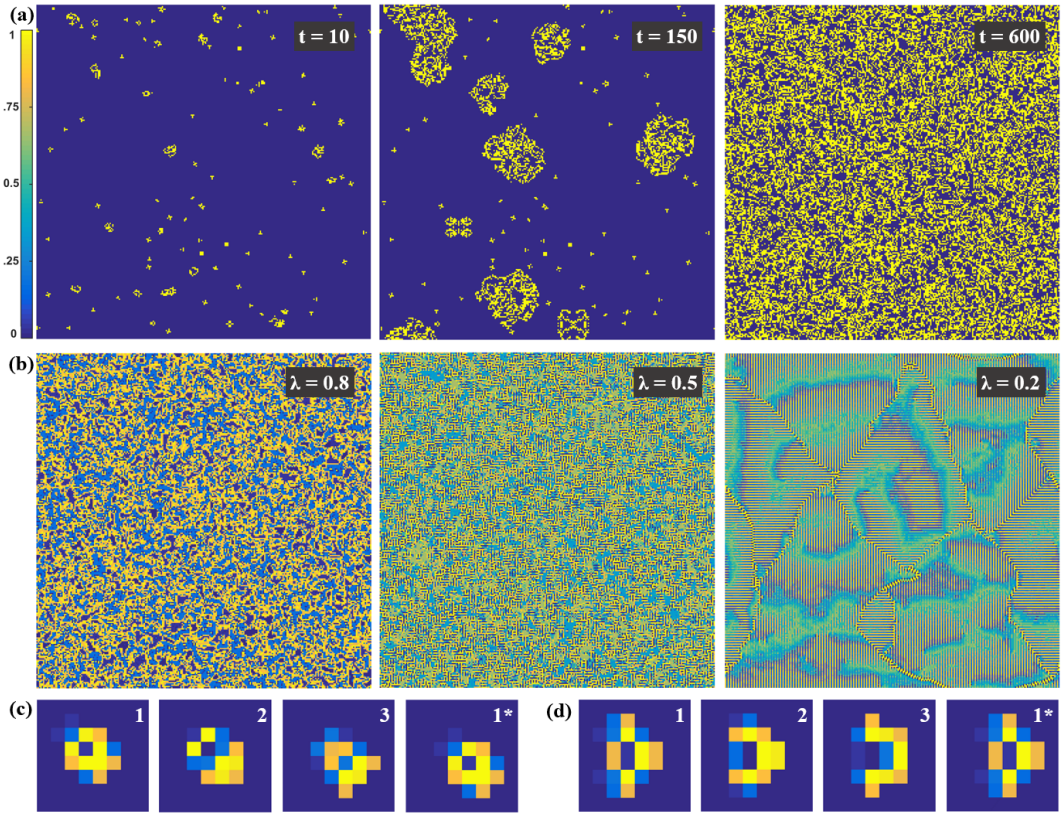

Figure 6.1: (a) Snapshots of 34 Life at three different time steps, initialized with $\rho_0 = 0.1$ of random binary values in a 256×256 lattice. (b) Asymptotic states of the same initial conditions at different λ values. Below: Structures and steps of an existing diagonal (c) and an emanating orthogonal (d) propagator at $\lambda = 0.8$ (see text).

In the Eq. 6.2 we notice the presence of growth and decay operations only. We run the system with a low initial density $\rho_0 = 0.1$ and observe how the complex structures quickly emerge, as shown in Fig. 6.1(a). Along, there are "seeds" of activity that have an expanding character and cover the whole cellular space in a relatively short transient time. We depart from $\lambda = 1$ to apply the logistic extension and observe how the tuning parameter redirects the dynamics into a different behavior. At $\lambda = 0.8$ the system shows a relatively similar behavior, with disordered regions of high activity. As the parameter is tuned more, the system starts showing qualitative changes where correlations start appearing in between the chaotic flickers (see Fig. 6.1(b)). Interestingly, at $\lambda = 0.2$ values, the correlations start supporting stripe like domains and the flickering chaotic sites get synchronized in a fashion that generates wave-like structures. In the asymptotic state, these waves keep periodically emerging and dissipating within the boundaries of stripe domains. We believe this is another exquisite example of self organized behavior.

Moreover, we observe emanating propagators, very similarly as in the Logistic GoL. The period-3 diagonal propagator shown in Figure 6.1(c) actually exists in the two-state version of 34 Life, and it preserves the shape and characteristics in a continuous range of λ, similarly with the Glider of GoL. However, there is an emerging propagator that only partially exists in 34 Life, and builds up step by step as λ is tuned. This structure is period-3, orthogonal and exists in a wide range of the parameter, yet much simpler when compared to the Rayfish in Logistic GoL. We believe that the emergent behavior present in this system will stimulate further examination of our framework into Life-Like rules which are mentioned in the literature.

6.2 Majority Rule

Majority rules are very common and simple rules introduced to model collective behavior of agents that follow the behavior of their neighbors, such as voting. We consider the logistic extension of a rule discussed by Chopard [11]. The cellular

space is square lattice and the interaction level is in the Moore neighborhood. The system is totalistic, which means that central sites are counted when calculating neighborhood sums. The state space is binary and the update equations for the twisted majority rule are:

$$s(\mathbf{r}, t+1) = \begin{cases} 1 \;\; ; & m(\mathbf{r}, t) = 0, 1, 2, 3, 5. \\ 0 \;\; ; & m(\mathbf{r}, t) = 4, 6, 7, 8, 9. \end{cases} \tag{6.3}$$

In the same fashion, it is obvious that there are only two operations present in the rules, namely growth and decay. We rewrite the finite difference form and define the new intervals based on the Eq. 6.3:

$$\Delta s = \begin{cases} \lambda(1-s) \; ; & m \leq 3.5, \; or \; 4.5 < m \leq 5.5. \\ -\lambda s \quad\;\; ; & 3.5 < m \leq 4.5, \; or \; m > 5.5. \end{cases} \tag{6.4}$$

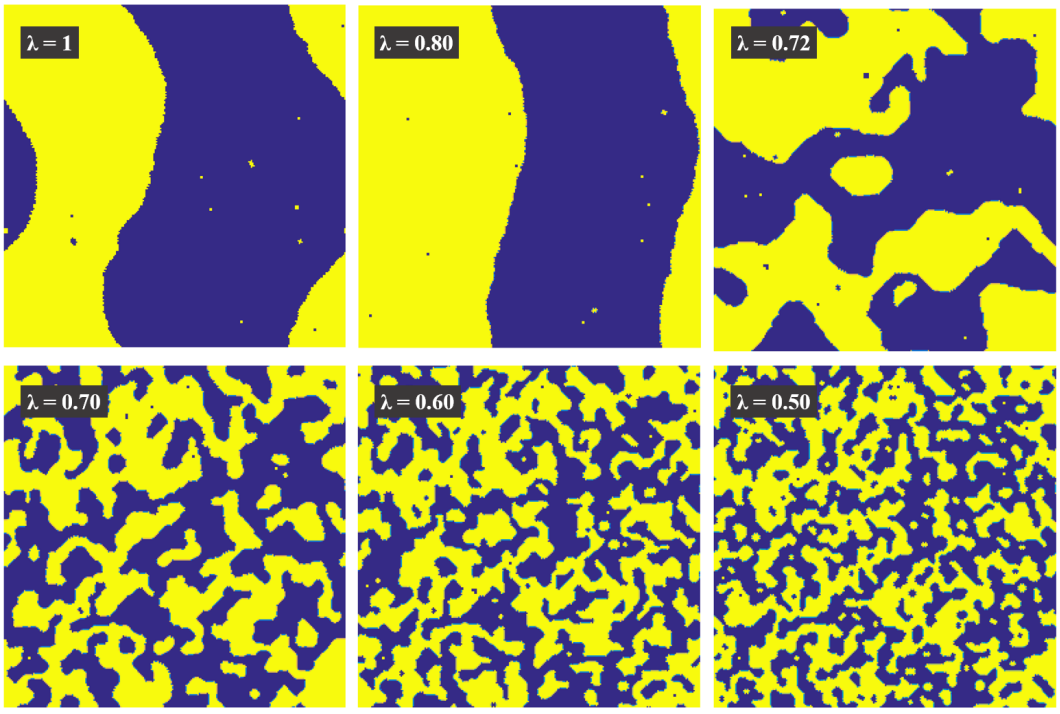

Figure 6.2: Asymptotic states of the majority rule (Eq. 6.4) run at six different λ values but with the same initial conditions, random distribution of binary values with a density $\rho_0 = 0.5$. Lattice size: 256×256; Iteration time: 10^4 steps.

A more realistic interpretation of the λ implementation would be: If agents are converging to their neighborhood majority at a lower rate, how would the overall dynamics of both phases change? Figure 6.2 shows how the dynamics of this system is influenced at different rates of change. Initially ($\lambda = 1, 0.8$) the collective behavior of interface motion is preserved and the perimeter formed by the boundaries of two phases stabilizes to a minimum length, and the phases become totally separated. However, as λ is tuned down, the perimeter stabilizes faster at more complex configurations and the phase separation instead is exhibited through a different interface dynamics. At $\lambda = 0.72$ we observe a "sharp" change in interface dynamics that becomes more and more complex as the parameter is tuned. At low ranges, both phases are stable and rather mixed throughout the cellular space.

6.3 Larger than Life

In this section, we introduce the logistic version of two automata that are part of the LtL family, discussed by Evans. [25]. The frameworks are defined in a 2D square lattice and rules represented by a 5-tuple of parameters $(\phi, \beta_1, \beta_2, \delta_1, \delta_2)$, where ϕ is the radius of neighborhood, β_1, β_2 and δ_1, δ_2 are the respective limits of birth and survival neighborhood sum limits, respectively. That is, a dead site will grow in the next time step if it's neighborhood sum is an integer between β_1 and β_2, included. And a live site will survive in the next time step if if it's neighborhood sum is an integer between δ_1 and δ_2, included. The neighborhood here covers a square of 121 sites. It is defined as totalistic, so we take this into account when rewriting the rules in the finite difference form.

The first model, $(5, 9, 9, 9, 10)$, is represented in the following fashion with an outer totalistic neighborhood (excluding central site from the sum):

$$\Delta s = \begin{cases} \lambda(1-s) \; ; \; 8.5 < m \leq 9.5. \\ 0 \qquad\quad ; \; 7.5 < m \leq 8.5. \\ -\lambda s \qquad ; \; 7.5 \leq m \; or \; m > 9.5. \end{cases} \tag{6.5}$$

The Δs transformation consists of the same equations of Logistic GoL, where the stability operation is also present as shown in Eq. 6.5 . $\lambda = 1$ generates the same dynamics of LtL rule introduced in the paragraph above. Figure 6.3 shows how the dynamics changes as the parameter is tuned. This rule is known to generate a sparse asymptotic behavior in which only a few propagators emerge and survive out of random initial conditions (see Fig. 6.3(a)). As λ is tuned down to 0.75, the activity increases and the local interactions of prior propagators decouple. The system becomes less sparse and highly disordered, and this activity starts getting more correlated as the parameter is tuned further.

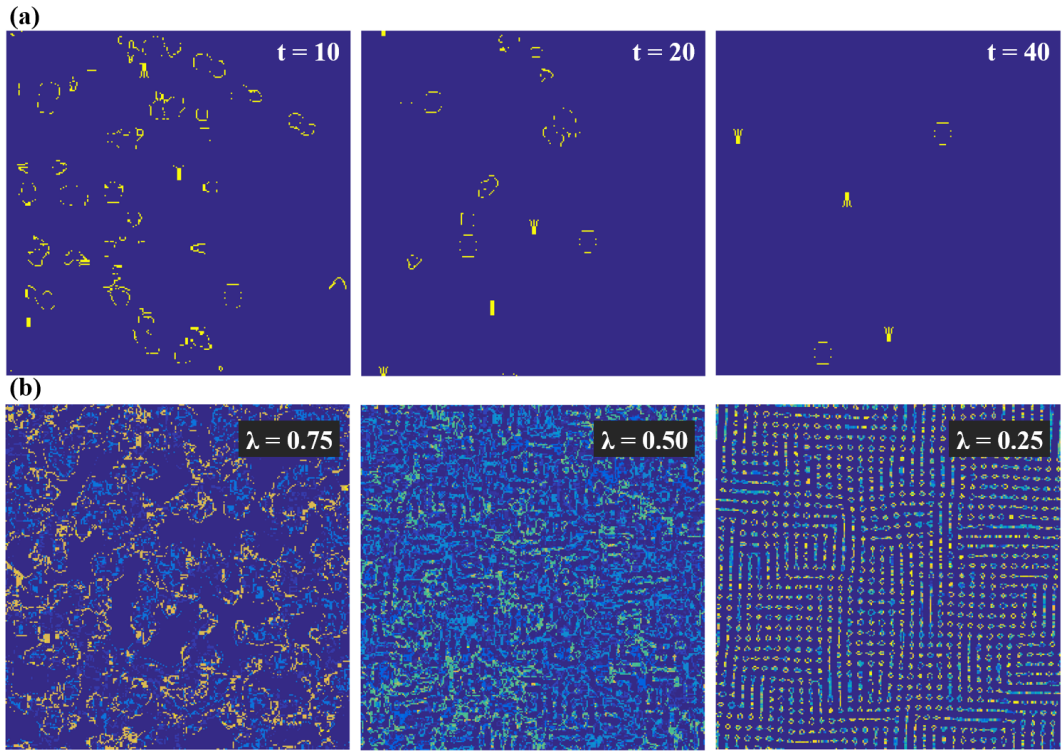

Figure 6.3: (a) Time evolution of LtL $(5, 9, 9, 9, 10)$ rule run at random initial binary values with $\rho_0 = 0.1$ in a 256×256 lattice. (b) Asymptotic behavior of the logistic version rewritten in Eq. 6.5 at three different λ values, iterated 300 time steps.

This activity eventually settles at low λ values where the system starts supporting a regular lattice of stable and oscillating structures that have very low amounts of interaction between each other (see Fig. 6.3(b)). This is another example where the system undergoes a transition and interactions can generate a wide variety of correlated structures that has actually a much higher density than before. Lower rate of growth and decay "allow" the local interactions to explore different types of nonlinear relations between sites. Structures and dense configurations similar with the ones in $\lambda = 0.2$ might be reachable with different rules, but it is quite interesting to observe them emerging in a model where the growth and stability regions are very narrow. Each of them covers less than 1% of the whole neighborhood interval that defines the regimes of operations.

Another interesting 5-tuple of rules in the LtL family is $(5, 34, 45, 34, 58)$ that supports a huge variety of bugs, oscillators and propagators. The rule is chaotic, yet the dominance of quiescent phase offers a proper environment for interactions of the complex structures (see Fig 6.4). We rewrite the respective rules in a finite difference form:

$$\Delta s = \begin{cases} \lambda(1-s) \; ; \; 33.5 < m \leq 45.5. \\ 0 \quad\quad\quad ; \; 32.5 < m \leq 33.5 \; or \; 45.5 < m \leq 58.5. \\ -\lambda s \quad\quad ; \; 32.5 \leq m \; or \; m > 58.5. \end{cases} \tag{6.6}$$

The Influence of the tuning parameter is qualitatively similar with that in the Logstic GoL case. The activity starts increasing and percolating throughout the whole lattice and disordered flickering phase dominates over the quiescent phase as λ is taken down to 0.85. Further tuning enables the system to reach into a regime that supports regular domains of orthogonal stripes that get organized and help generate each other through correlations, as shown for $\lambda = 0.70$.

Interestingly, in this system we also notice the emergence of a homogeneous period-2 flickering phase. They are collective oscillations of sites that emerge from random initial conditions, the 2D counterpart of stripes observed in logistic Rule 90. In this case, despite a wider neighborhood, every flickering site has a

neighborhood with the same states and a sum m that oscillates between decay and growth regimes indefinitely. The snapshot representing the system at $\lambda = 0.55$ is not necessarily an asymptotic state. Both phases, stripes and periodic flickers, are in a consistent competition and often one prevails over the other.

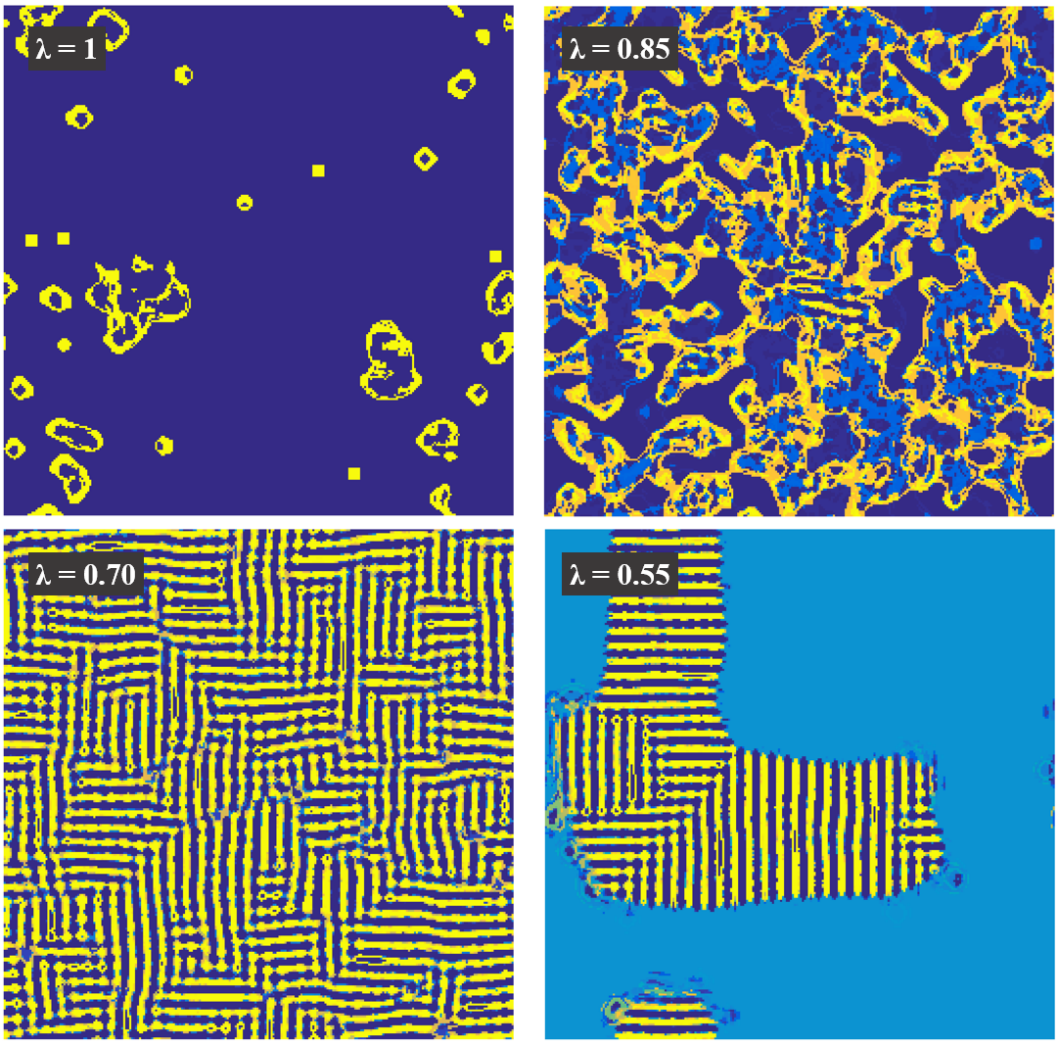

Figure 6.4: Asymptotic behavior of the logistic version of LtL $(5, 34, 45, 34, 58)$ rule rewritten in Eq. 6.6 at four different λ values. Initial conditions are random distribution of binary values with $\rho_0 = 0.5$ in a 256×256 lattice, iterated 300 time steps.

6.4 Outlook

In this study, aiming to re-emphasize the importance of CA as proper tools for complex systems, we report a simple implementation of a parameter which tunes the decay/growth rate and in principle can be extended to any dimensional two-state totalistic model. Applying this parameter to Conway's GoL brings up a transformation of the state space into a Cantor set, and a series of deterministic phase transitions with the emergence of self-organized patterns. Moreover, we discuss how the same system can serve as a playground for the emergence of propagating spatio-temporal correlations under the influence of a single parameter. The tunable emanation of complex localized structures is a novel phenomenon in the spectrum of CA.

Meanwhile, the operation notation serves as a useful definition that provides tools for analysing the transition points and their self-similar nature when studying the asymtotic dynamics of systems. It is also extremely useful for quantifying the autocatalytic interaction sets. One can record all the operations of a complex structure and use the polynomial representation to define the parameter range of the existence of that structure and any information about its sites and stages.

The analysis of propagators or replicators as emergent phenomena, their development, adaptation or transformation over a continuous range of parameter is another focal point which contributes to understanding of autocatalytic loops in real chemical or biological systems and how they are affected by possible changes in exterior conditions. Continuous parameters such as temperature or chemical concentrations often are directly related to the rate of change of local internal processes of biologcal cycles, such as ATP hydrolysis or protein folding. Parameter tuned CA might serve as phenomenological simplified models to address such phenomena.

We also show that the logistic extension can induce interesting behavior even in a 1D system, Rule 90. Along with the critical transitions in dynamics, we report emergence of collectively oscillating states, generating phases of different

periods. Moreover, we observe the emergence of a propagator that also transforms into another propagator as the parameter is tuned. These events are at the same time related to transition in universality classes within the same system. These results will shed light on parameter tuned class transitions in CA and sharp phase transitions in deterministic systems, a question addressed earlier [50] but never with a parameter that can be varied continuously.

Bibliography

[1] J. von Neumann, Theory of Self-Reproducing Automata, edited and completed by A.W. Burks (University of Illinois Press, Urbana, IL, 1966).

[2] C. G. Langton, Proc. Vol. St. Fe Inst. Stud. Sci. Complex. v. 6 (1989).

[3] T. Toffoli and N. Margolus, Cellular Automata Machines: A New Environment for Modeling (MIT, Cambridge, Mass. , 1986).

[4] L. B. Kier, C. K. Cheng, and P. G. Seybold, SAR QSAR Environ. Res. **11**, 79 (2000).

[5] H. Seybold, J. S. Andrade, Jr., and H. J. Herrmann, Proc. Natl. Acad. Sci. U.S.A. **104**, 16804 (2007).

[6] R. White and G. Engelen, Environ. Plan. A Econ. Sp. **25**, 1175 (2006).

[7] C. Saloma, G. J. Perez, G. Tapang, M. Lim, and C. Palmes-Saloma, Proc. Natl. Acad. Sci. U. S. A. **100**, 11947 (2003).

[8] U. Frisch, B. Hasslacher, and Y. Pomeau, Phys. Rev. Lett. **56**, 1505 (1986).

[9] G. Y. Vichniac, Physica (Amsterdam) **10D**, 96 (1984).

[10] J. S. Langer, Rev. Mod. Phys. 52, **1** (1980).

[11] B. Chopard, in Comput. Complex. Theory, Tech. Appl. (2012), pp. 407-433.

[12] A. Deutsch and S. Dormann, in Model. Simul. Sci. Eng. Technol. (2017), pp. 1-464.

[13] L. Manukyan, S. A. Montandon, A. Fofonjka, S. Smirnov, and M. C. Milinkovitch, Nature **544**, 173 (2017).

[14] P. Bak, Ch. Tang, and K. Wiesenfeld, Phys. Rev. A **38**, 364.

[15] A. Ilachinski, Cellular Automata a Discrete Universe (World Scientific, Singapore, 2001).

[16] S. Wolfram, Nature **311**, 419 (1984).

[17] G. t'Hooft, *The Cellular Automaton Interpretation of Quantum Mechanics* in Fundamental Theories of Physics (Springer, New York, 2016), Vol. 185.

[18] T. Toffoli, Phys. D Nonlinear Phenom. **10**, 117 (1984).

[19] B. Chopard and M. Droz, Cellular automata modeling of physical systems, (Cambridge University Press, Cambridge, 1998).

[20] J.B.C. Garcia, M.A.F. Gomes, T.I. Jyh, T.I. Ren, and T.R.M. Sales, Phys. Rev. E **48**, 3345 (1993).

[21] L. S. Schulman and P. E. Seiden, J. Stat. Phys. **19**, 293 (1978).

[22] F. Bagnoli, R. Rechtman, and S. Ruffo, Phys. A Stat. Mech. Its Appl. **171**, 249 (1991).

[23] D. Eppstein, in Game Life Cell. Autom. (2010), pp. 71-97.

[24] A. C. De La Torre and H. O. Mártin, Phys. A Stat. Mech. Its Appl. **240**, 560 (1997).

[25] K. M. Evans, Phys. D Nonlinear Phenom. **183**, 45 (2003).

[26] D. J. Watts and S. H. Strogatz, Nature **393**, 440 (2002).

[27] S. Y. Huang, X. W. Zou, Z. J. Tan, and Z. Z. Jin, Phys. Rev. E **67**, 026107 (2003).

[28] J. Nordfalk and P. Alstrøm, Phys. Rev. E **54**, R1025 (1996).

[29] H. J. Blok and B. Bergersen, Phys. Rev. E **59**, 3876 (1999).

[30] S. M. Reia and O. Kinouchi, Phys. Rev. E **89**, 052123 (2014).

[31] P. Bak, K. Chen, and M. Creutz, Nature **342**, 780 (1989).

[32] C. Bays, Complex Syst. **15**, (2005) pp. 245–252.

[33] C. Bays, Complex Syst. **1**, 373 (1987).

[34] S. Wolfram, A New Kind of Science, (Wolfram Media, Champaign, IL, 2002).

[35] S. Wolfram, Los Alamos Science **9**, 2-21 (1983).

[36] R. M. May, Nature **261**, 459 (1976).

[37] S. H. Strogatz, Nonlinear Dynamics And Chaos: With Applications To Physics, Biology, Chemistry, And Engineering, Studies in Nonlinearity (Westview Press, Perseus Books Group, Cambridge, 2001).

[38] K. Kaneko, Chaos **2**, 279 (1992).

[39] H. Chaté and P. Manneville, J. Stat. Phys. **56**, 357 (1989).

[40] S. Wolfram, Rev. Mod. Phys. **55**, 601 (1983).

[41] P. Rendell, in Des. Beauty Art Cell. Autom., edited by A. Adamatzky and G. J. Martínez (Springer International Publishing, Cham, 2016), pp. 149-154.

[42] M. Hurley, Ergod. Th. Dynam. Syst. **10**, 131 (1990).

[43] S. A. Kauffman, The Origins of Order: Self-Organization and Selection in Evolution (Oxford University Press, New York, 1993).

[44] E. Bilotta and P. Pantano, in Cell. Autom. Complex Syst., edited by E. F. Codd (Academic Press, 2010), pp. 17-50.

[45] O. Martin, A. M. Odlyzko, and S. Wolfram, Commun. Math. Phys. **93**, 219 (1984).

[46] T. Y. Li and J. A. Yorke, Am. Math. Mon. **82**, 985 (1975).

[47] C. G. Langton, Phys. D Nonlinear Phenom. **42**, 12 (1990).

[48] Eldredge N, Gould SJ (1972) Punctuated equilibria: An alternative to phyletic gradualism. *Models in Paleobiology* , ed Schopf TJM (Freeman, Cooper and Company, San Francisco), pp 82-115.

[49] P. Bak and K. Sneppen, Phys. Rev. Lett. **71**, 4083 (1993).

[50] W. K. Wootters and C. G. Langton, Phys. D Nonlinear Phenom. **45**, 95 (1990).